Table 3 List of the miRNAs used to classify patients into R and NR groups

Gene name	fold change (R/NR)	T-test	Selection by MCCV		
			Rank	appearance frequency in this classification (%)	appearance number of times
hsa-miR-122a	1.50	6.70E-02	1	98.57	690
hsa-miR-21	1.13	5.43E-01	2	89.86	629
hsa-let-7a	1.15	4.23E-01	3	88.71	621
hsa-let-7f	1.24	3.01E-01	4	87.43	612
hsa-miR-148a	1.70	4.51E-02	5	82.71	579
hsa-miR-192	1.24	1.93E-01	6	81.71	572
hsa-miR-126	1.21	3.19E-01	7	74.14	519
hsa-miR-22	1.04	7.88E-01	8	68.43	479
hsa-miR-194	1.20	3.63E-01	9	64.29	450
hsa-miR-23b	1.30	2.06E-01	10	62.00	434
hsa-miR-125b	1.23	2.88E-01	11	61.86	433
hsa-miR-494	0.45	8.17E-02	12	61.14	428
hsa-miR-19b	1.17	3.86E-01	13	61.14	428
hsa-miR-29a	1.11	5.44E-01	14	59.86	419
hsa-miR-26a	1.13	5.38E-01	15	58.43	409
hsa-let-7b	1.01	9.37E-01	16	56.86	398
hsa-miR-142-3p	1.15	5.54E-01	17	52.71	369
hsa-miR-215	1.28	3.93E-01	18	52.00	364
hsa-miR-101	1.31	1.26E-01	19	49.00	343
hsa-miR-451	1.35	5.25E-01	20	48.14	337
hsa-miR-145	0.99	9.76E-01	21	47.14	330
hsa-let-7g	1.15	4.84E-01	22	44.00	308
hsa-miR-29c	1.23	2.94E-01	23	43.71	306
hsa-miR-26b	1.37	2.85E-01	24	43.14	302
hsa-miR-768-3p	1.00	9.91E-01	25	36.29	254
hsa-let-7c	1.16	3.76E-01	26	36.14	253
hsa-miR-370	0.43	7.36E-02	27	35.57	249
hsa-miR-92	1.07	6.65E-01	28	34.14	239
hsa-miR-16	1.11	6.18E-01	29	26.71	187
hsa-miR-29b	1.14	5.19E-01	30	25.71	180
hsa-miR-27b	1.40	1.15E-01	31	25.71	180
hsa-miR-24	1.08	6.56E-01	32	20.57	144
hsa-miR-107	1.00	9.81E-01	33	19.57	137
hsa-miR-143	0.95	7.99E-01	34	18.43	129
hsa-miR-214	0.85	3.61E-01	35	17.86	125

the miRNAs that were associated with the drug response to the combination therapy, we chose miRNAs which had ≥ 1.25 fold difference in the mean values of the gene expression level between at least two groups ($p < 0.05$). Unsupervised hierarchical clustering based on all the miRNAs spotted on the chip, revealed a marked, very distinct separation according to the patients' final response of the CHC liver tissue to the Peg-IFN and ribavirin combination therapy (Figure 2).

The result was that the expression level of 3 miRNAs (miR-27b, miR-378, miR-422b) in SVR was significantly higher than that in NR, whereas the expression level of 5 miRNAs (miR-34b, miR-145, miR-143, miR-652, and miR-18a) in SVR was significantly lower than that in NR. Without FDR correction, the expression level of miR-122 in NR was lower than that in SVR. The expression level of 2 miRNAs in SVR was significantly higher than that in R, whereas the expression level of 10 miRNAs in SVR was significantly lower than in that in R. Additionally, the expression level of miR-148a in R was significantly higher than that in NR. There was no significant difference in the expression level of miR-122 in NR and R (Table 4).

Validation of the microarray result by real-time qPCR

The three miRNAs (miR-18a, miR-27b, and miR-422b) with the smallest difference of fold change between NR and SVR groups and four miRNA (miR-143, miR-145,

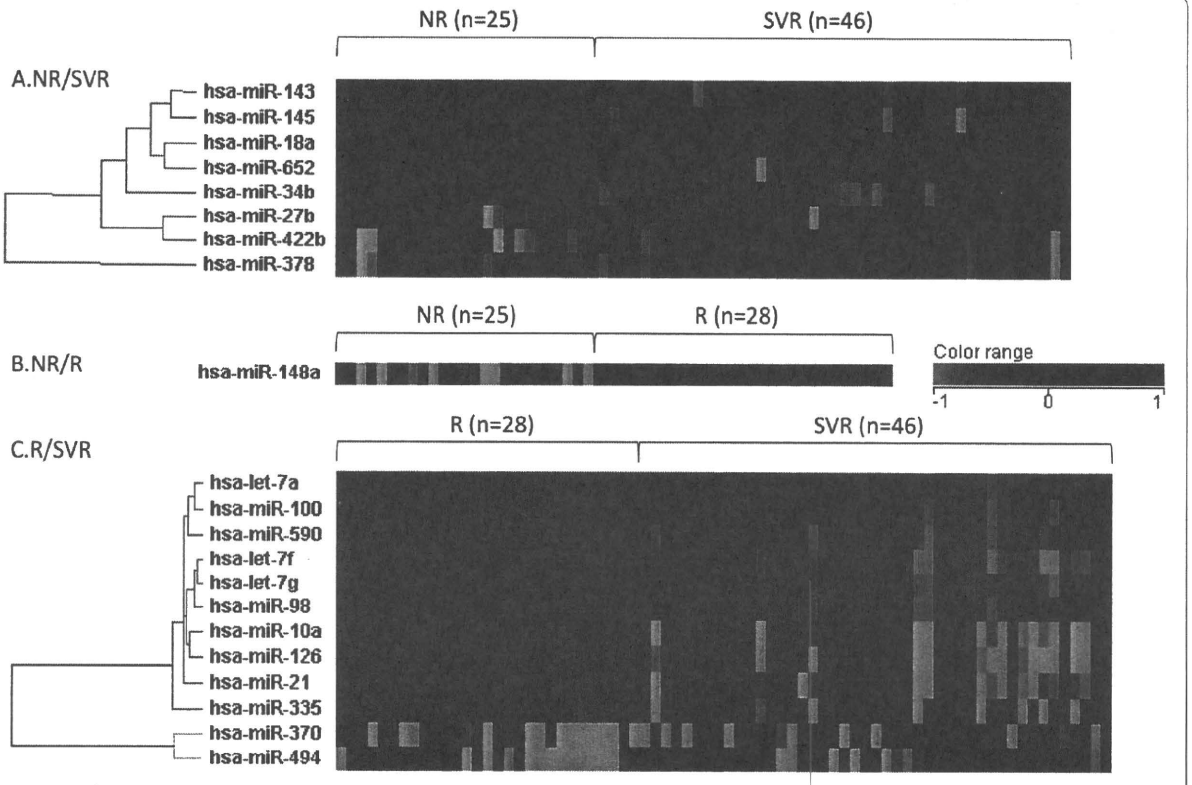

Figure 2 Clustering of CHC patients according to their final response to Peg-IFN and ribavirin combination therapy. Heatmap using miRNA differently expressed among SVR, R, and NR is shown (A: classification between NR and SVR, B: classification between NR and R, and C: classification between R and SVR, respectively). Vertical bars represent the miRNA genes and the horizontal bars represent the samples. Green bars reflect downregulated genes and red bars upregulated genes.

miR-34b, and miR-378) with the largest difference of fold change between NR and SVR groups were chosen to confirm the microarray results using stem-loop based real-time qPCR. The result of real-time qPCR corresponded to the result from the microarray analysis (Figure 3).

miRNAs which related to the 4 week (rapid response phase) response to combination therapy

The miRNA expression profile was established according to the rapid phase response to the combination therapy by week 4 (Table 5). Our results showed that the expression level of 5 miRNAs in non-RVR was significantly higher than that in RVR. Prior results have revealed that a patient who achieves RVR as a result of the combination therapy has a high possibility of achieving SVR [22,23]. Our research supports this finding: nine out of 99 patients achieved RVR. All nine cases shifted to cEVR by week 12, and 8 shifted to SVR at the final response. The 90 cases in non-RVR shifted to 44 cases in cEVR, 19 in pEVR, and 27 in non-EVR and at the final response shifted to 38 cases in SVR, 27 in R, and 25 in NR (Table 6 and Figure 1).

miRNAs which related to the 12 week (early response phase) response to combination therapy

Establishing the miRNA expression profile of patients according to their 12 week (early response) of CHC liver specimen to the combination therapy after 12 weeks, showed that the expression level of miR-23b and miR-422b in cEVR was higher than that in non-EVR, and the expression level of miR-34b in cEVR lower than that in non-EVR (Table 5). There were no miRNAs with expression level that differed significantly between cEVR and pEVR, and non-EVR and pEVR. The drug response at 12 weeks appeared to be a predictive factor of the final drug response. The 53 cases in cEVR at week 12 shifted to 41 cases in SVR and 12 in R at the final response. 27 cases in pEVR at week 12, shifted to 5 in SVR, 15 in R, and 7 in NR and 19 in non-EVR shifted to 1 in R and 18 in NR (Table 6 and Figure 1).

Predicting the final outcome before drug administration using MCCV

Before initial drug administration, we attempted to simulate the clinical outcome of the combination

Table 4 Extracted miRNA related to the final outcome of combination therapy

Gene Name	Fold Change (NR/SVR)	p-value with FDR correction	p-value without correction
hsa-miR-34b*	1.50	3.53E-02	6.95E-05
hsa-miR-145	1.35	3.55E-02	5.50E-05
hsa-miR-143	1.31	4.65E-02	6.46E-04
hsa-miR-652	1.28	4.33E-02	3.43E-04
hsa-miR-18a	1.22	4.33E-02	2.02E-05
hsa-miR-27b	0.78	4.33E-02	3.97E-05
hsa-miR-422b*	0.71	4.33E-02	1.44E-04
hsa-miR-378	0.70	4.86E-02	1.38E-03
hsa-miR-122	0.72	> 5.00E-02	2.59E-04

Gene Name	Fold Change (NR/R)	p-value with FDR correction	p-value without correction
hsa-miR-148a	0.59	1.60E-02	8.99E-04
has-miR-122	0.72	> 5.00E-02	6.23E-04

Gene Name	Fold Change (R/SVR)	P-value	p-value without correction
hsa-let-7a	1.15	3.93E-02	1.94E-03
hsa-let-7f	1.24	1.04E-02	3.60E-03
hsa-let-7g	1.17	1.93E-02	1.82E-02
hsa-miR-100	1.23	1.93E-02	9.23E-04
hsa-miR-10a	1.37	1.26E-02	2.40E-03
hsa-miR-126	1.36	1.04E-02	1.50E-03
hsa-miR-21	1.30	4.78E-02	3.45E-02
hsa-miR-335	2.00	2.83E-02	3.50E-02
hsa-miR-370	0.36	1.38E-02	2.96E-03
hsa-miR-494	0.37	3.93E-02	1.97E-03
hsa-miR-590	1.26	3.93E-02	5.59E-03
hsa-miR-98	1.22	1.38E-02	6.64E-03

Asterisk was denoted the common miRNAs appeared whose expression level between NR and SVR, and nonEVR and cEVR.

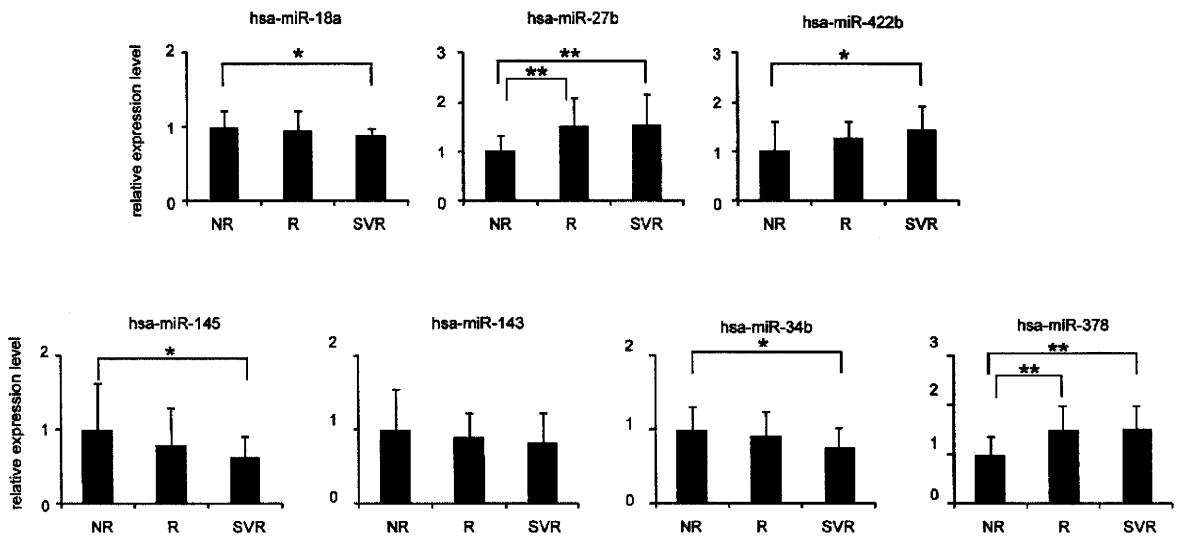

Figure 3 Real-time qPCR validation of the seven miRNAs. Each column represents the relative amount of miRNAs normalized to expression level of U18. The data shown were means+SD of three independent experiments. Asterisk indicates a significant difference of $p < 0.05$ (*) or $p < 0.01$ (**).

Table 5 List of the miRNA related to the rapid or early outcome of combination therapy

Gene Name	Fold Change (non RVR/RVR)	p-value	p-value without correction
hsa-let-7c	1.17	2.01E-02	8.31E-03
hsa-let-7d	1.13	3.50E-02	5.63E-02
hsa-miR-139	1.29	3.35E-02	2.70E-02
hsa-miR-324-5p	1.14	1.64E-02	3.24E-02
hsa-miR-768-5p	1.34	4.57E-02	1.29E-02

Gene Name	Fold Change (non EVR/cEVR)	p-value	p-value without correction
hsa-miR-34b*	1.51	3.30E-02	1.69E-04
hsa-miR-23b	0.74	2.69E-02	8.91E-05
hsa-miR-422b*	0.67	2.40E-02	1.34E-04
hsa-miR-122	0.74	> 5.00E-02	3.07E-03

Asterisk was denoted the common miRNAs appeared whose expression level between NR and SVR, and nonEVR and cEVR.

therapy before drug administration by using MCCV. We first extracted the SVR and non-SVR groups from all of the patients, and then the R and NR groups were predicted afterwards. MCCV simulation showed that the accuracy, specificity, and sensitivity of the liver specimen classified as SVR or non-SVR was up to 70.5%, 63.3%, and 76.8%, respectively (TSs = 80). On the other hand, the accuracy, specificity, and sensitivity of the liver specimen classified as R or NR was 70.0%, 73.7%, and 67.5%, respectively (TSs = 42)(Figure 4). Fold change of their normalized expression level, P value, and number of selection by MCCV in the 35 informative miRNAs that were identified based on the all patients are shown in Table 2 and 3.

miRNAs related to the final drug response can regulate the immune related genes

In order to clarify the biological links between miRNAs and IFN responses, we examined whether the expression of immune-related hypothetical miRNAs target genes (additional file 1) could be controlled by miRNAs which were related to the final drug response. We observed the changes in expression level of B-cell CLL/lymphoma 2 (BCL2), retinoic acid receptor, alpha (RARA), and SMAD family member 2 (SMAD2) by real-time qRT-PCR as the expression level of miRNAs (miR-143, miR-27b, and miR-18a) was modified, respectively, in HEK293 cells. The expression level of the hypothetical targets examined was down-regulated by over-expression of the corresponding miRNA and the corresponding antisense oligonucleotide (ASO) inhibited the function of miRNA (additional file 2).

Discussion

Our large and comprehensive screening revealed that hepatic miRNA expression can be associated with a patient's drug response. There are several reports that miRNAs are closely related to innate immunity, and in this study, we found that several miRNAs had the potential to recognize immuno-related genes as target candidates [24-26]. For example, the following hypothetical candidate genes of miR-378, miR-18a, miR-27b, miR-34b, and miR-145 each identified as target genes, Interferon Response Factor (IRF) 1, IRF2, IRF4, IRF6, and IRF7, respectively (additional file 1). Past reports show that miR-422b was related to the B cell differentiation [27]. When an immuno-reaction induces aberrant expression of miRNA, the expression level of miR-34b significantly decreased in H69 cells following IFN-γ stimulation [28]. Bcl-6 positively directs follicular helper T cell differentiation, through combined repression of miR-18a and miR-27b and transcription factors [29].

In our study, there was significant difference in the fold change of the expression level of miRNA based on the drug response, however, the absolute value of the fold change was not so significant (Table 4). Usually one miRNA can regulate many genes including immuno-related gene (additional file 1), and these genes in turn can synergistically affect immune activity. In our preliminary study (additional file 2) BCL-2, RARA, and SMAD2 can be regulated by miR-143, miR-18a, and miR-27b, respectively. Considering that the expression level of several miRNAs changed these minute changes taken together can have a significant impact on a patient's drug-response and innate immunity.

Aberrant expression of miRNA can modify the replication of HCV. According to Vita algorithm, several miRNAs, related to drug response, can recognize HCV genotype 1b sequence as a target (additional file 3) [30]. For example, miR-199a* is able to target the HCV genome and inhibit viral replication [12]. IFN has the ability to modulate expression of certain miRNAs that may either target the HCV RNA genome (miR-196 or miR-

Table 6 Patients' periodical drug response changes

code No.	4W treatment (rapid response)	12W treatment (early response)	48W treatment +24W observation (final outcome)	code No	4W treatment (rapid response)	12W treatment (early response)	48W treatment +24W observation (final outcome)
OCH-105	non RVR	non EVR	NR	OCH-103	RVR	cEVR	SVR
OCH-111	non RVR	pEVR	NR	OCH-104	non RVR	cEVR	SVR
OCH-118	non RVR	non EVR	NR	OCH-107	non RVR	cEVR	SVR
OCH-119	non RVR	non EVR	NR	OCH-108	non RVR	cEVR	SVR
OCH-122	non RVR	pEVR	NR	OCH-109	non RVR	cEVR	SVR
OCH-123	non RVR	non EVR	NR	OCH-110	non RVR	cEVR	SVR
OCH-126	non RVR	non EVR	NR	OCH-112	non RVR	pEVR	SVR
OCH-127	non RVR	non EVR	NR	OCH-114	RVR	cEVR	SVR
OCH-132	non RVR	pEVR	NR	OCH-116	non RVR	cEVR	SVR
OCH-137	non RVR	non EVR	NR	OCH-121	non RVR	pEVR	SVR
OCH-140	non RVR	pEVR	NR	OCH-124	non RVR	cEVR	SVR
OCH-142	non RVR	non EVR	NR	OCH-130	non RVR	cEVR	SVR
OCH-144	non RVR	pEVR	NR	OCH-131	non RVR	cEVR	SVR
OCH-145	non RVR	non EVR	NR	OCH-136	non RVR	cEVR	SVR
OCH-192	non RVR	non EVR	NR	OCH-138	non RVR	cEVR	SVR
OCH-204	non RVR	non EVR	NR	OCH-139	non RVR	cEVR	SVR
OCH-205	non RVR	non EVR	NR	OCH-143	non RVR	cEVR	SVR
OCH-206	non RVR	non EVR	NR	OCH-150	non RVR	cEVR	SVR
OCH-207	non RVR	non EVR	NR	OCH-153	non RVR	cEVR	SVR
OCH-208	non RVR	non EVR	NR	OCH-154	non RVR	cEVR	SVR
OCH-209	non RVR	pEVR	NR	OCH-155	non RVR	cEVR	SVR
OCH-210	non RVR	non EVR	NR	OCH-156	non RVR	cEVR	SVR
OCH-211	non RVR	non EVR	NR	OCH-157	non RVR	pEVR	SVR
OCH-223	non RVR	non EVR	NR	OCH-158	non RVR	pEVR	SVR
OCH-242	non RVR	pEVR	NR	OCH-160	non RVR	cEVR	SVR
OCH-101	non RVR	cEVR	R	OCH-186	non RVR	cEVR	SVR
OCH-102	RVR	cEVR	R	OCH-187	non RVR	cEVR	SVR
OCH-106	non RVR	non EVR	R	OCH-189	non RVR	pEVR	SVR
OCH-113	non RVR	pEVR	R	OCH-190	non RVR	cEVR	SVR
OCH-115	non RVR	cEVR	R	OCH-191	RVR	cEVR	SVR
OCH-117	non RVR	cEVR	R	OCH-194	non RVR	cEVR	SVR
OCH-120	non RVR	pEVR	R	OCH-195	non RVR	cEVR	SVR
OCH-125	non RVR	pEVR	R	OCH-222	non RVR	cEVR	SVR
OCH-128	non RVR	pEVR	R	OCH-228	non RVR	cEVR	SVR
OCH-129	non RVR	pEVR	R	OCH-229	RVR	cEVR	SVR
OCH-133	non RVR	pEVR	R	OCH-230	non RVR	cEVR	SVR
OCH-134	non RVR	pEVR	R	OCH-231	non RVR	cEVR	SVR
OCH-135	non RVR	cEVR	R	OCH-232	non RVR	cEVR	SVR
OCH-141	non RVR	cEVR	R	OCH-233	non RVR	cEVR	SVR
OCH-151	non RVR	pEVR	R	OCH-234	RVR	cEVR	SVR
OCH-152	non RVR	pEVR	R	OCH-236	non RVR	cEVR	SVR
OCH-159	non RVR	pEVR	R	OCH-237	non RVR	cEVR	SVR
OCH-188	non RVR	cEVR	R	OCH-238	non RVR	cEVR	SVR
OCH-213	non RVR	cEVR	R	OCH-240	RVR	cEVR	SVR
OCH-214	non RVR	pEVR	R	OCH-241	RVR	cEVR	SVR
OCH-215	non RVR	pEVR	R	OCH-243	RVR	cEVR	SVR
OCH-216	non RVR	cEVR	R				
OCH-217	non RVR	pEVR	R				
OCH-218	non RVR	cEVR	R				

Table 6: Patients?'? periodical drug response changes *(Continued)*

OCH-219	non RVR	pEVR	R
OCH-220	non RVR	cEVR	R
OCH-221	non RVR	pEVR	R
OCH-239	non RVR	cEVR	R

448) or markedly enhance its replication (miR-122) [10,11]. The low expression level of miR-122 in the subjects shown in the NR group is in accordance with our results, however, after miRNA expression profile with FDR correction, the expression level of miR-122 was not significantly different between SVR and NR groups [8]. One reason why this difference is that their study comprised of patients infected with HCV genotype from 1 to 4 while this study consisted of HCV genotype 1b patients only.

The expression pattern of mRNA in HCV infected liver tissue is different from that of healthy tissue [15]. The expression pattern of the IFN-related genes in liver tissue before administering of IFN therapy, also differs according to the drug response [15,19]. The amount of plasmacytoid dendritic cell (pDC), which are the most potent secretors of antiviral Type-I IFN, has been shown to decrease in the peripheral blood of patients, however, pDC tend to become trapped in the liver tissue if HCV infection is present [31,32]. Taken together, it is possible that the variation in the miRNA expression pattern according to the drug response existed even before therapy.

Previously, large randomized controlled trials of IFN therapy for CHC, identified at pre-treatment stage several possible factors which are associated with the final virological response. These factors include: genotype, amount of HCV RNA in peripheral blood, degree of fibrosis, age, body weight, ethnicity, and steatosis [33]. Viral genome mutation in the ISDR region and the

A

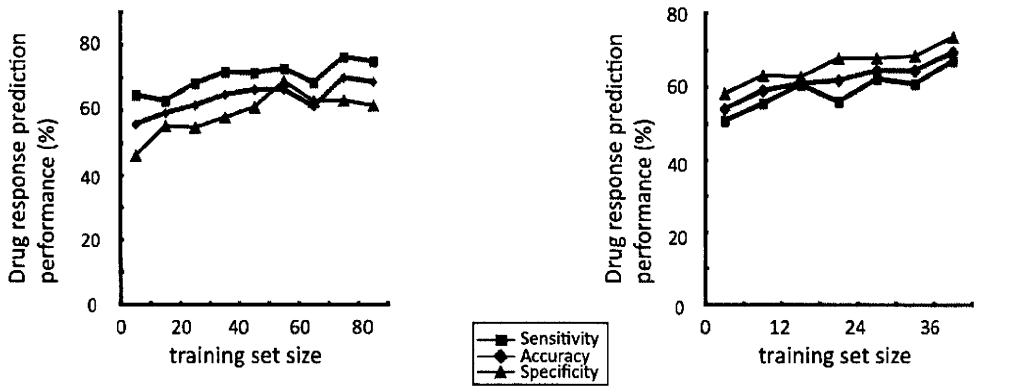

B

Training	Validation	Accuracy(%)	Sensitivity(%)	Specificity(%)	miRNA_Number
10	89	56.10	65.06	46.31	23
20	79	59.54	63.32	55.38	34
30	69	62.00	68.61	54.91	14
40	59	65.22	72.09	57.93	17
50	49	66.80	71.92	61.12	17
60	39	66.77	73.26	69.07	15
70	29	61.72	68.98	62.99	30
80	19	70.47	76.82	63.31	18
90	9	69.22	75.52	61.72	18

Training	Validation	Accuracy(%)	Sensitivity(%)	Specificity(%)	miRNA_Number
6	48	54.31	51.03	58.29	5
12	42	59.33	55.75	63.24	22
18	36	61.31	60.87	62.87	34
24	30	62.23	56.31	68.07	11
30	24	64.96	62.52	68.09	18
36	18	64.89	61.17	68.69	24
42	12	70.00	67.53	73.73	26

Figure 4 Method for predicting the clinical outcome using MCCV. Prediction performance of signatures from 35 miRNAs (Table 2 and 3). Left: Mean accuracy, specificity, and sensitivity (% in vertical axis) as a function of the training set size were determined for the 100 random splits of patients (non-SVR (NR+R) vs. SVR). Right: prediction performance of the training set size was determined by performing 48 random splits of patients (NR vs. R). A. Prediction performance (mean accuracy, specificity, and sensitivity) and number of miRNAs which was used for the prediction are also shown in each training set (TS) and validation set (VS).

substitutions of amino acid in the HCV core region also served as predictors of early, as well as end-of treatment response [13,14]. The miRNA expression obtained from the therapeutic response, can be applied to the prediction of drug response. The advantages of using miRNA for the microarray analysis include the following; (i) It was relatively easy to analyze because fewer probes were installed compared with the usual cDNA array. (ii) The change in each manifestation of a miRNA was low, in fact, in most miRNA, standard deviation was twice or less in average value (data not shown). The expression levels of miR-34b and 422b in the early response phase and final responses to treatment were consistently and significantly high and low in non-responders, respectively. Therefore these two miRNAs may be useful markers for early-to-final drug response to the IFN treatment.

Further studies are indeed needed to clarify the connection between miRNA expression and patient response to CHC combination therapy. Because information on miRNA is regularly being updated, we are planning to performed more analysis using the latest microarray and a larger sample in the future. However, in the meantime, as we have shown in Figure 4, the bigger the size of the training set, the higher the prediction performance that is achieved. This combined with the results of our Monte Carlo cross validation provided a strong based to verify the concepts in this report. We believe that our results have three advantages (i) the prediction methods used were quite reasonable, (ii) the prediction performance can later be improved if more patients' data become available and (iii) obtaining miRNA profile (not specific miRNAs) is useful for predicting the drug response. While current therapy is based on positive selection with HCV genotype or negative selection with IL28B SNP, and is limited to only some cases, our methods are applicable to all patients [13,18].

Conclusions

Our study shows that the specific miRNA are expressed differently depending on patient's drug response. As result we feel that miRNA profiling can be useful for predicting patient drug response before the administering combination therapy thereby reducing ineffective treatments. Moreover, miRNA expression profile can facilitate the accumulation of basal information for the development of novel therapeutic strategies. This approach allows for more suitable therapeutic strategies based on clinical information of individuals.

Additional material

Additional file 1: miRNA hypothetical target genes according to in silico analysis.

Additional file 2: Real-time qPCR validation of immune-related hypothetical target genes of miRNAs. The expression levels of hypothetical target genes in HEK293 cells were compared among three groups treated with control RNA, ds miRNA, and ASO miRNA. The data shown are means+SD of three independent experiments. Asterisk indicates a significant difference of $p < 0.05$.

Additional file 3: human miRNA target on the HCV genome genotype 1b (Accession No. AF333324)

List of abbreviations

HCV: hepatitis C virus; CH: chronic hepatitis C; LC: liver cirrhosis; HCC: hepatocellular carcinoma; miRNA: microRNA; IFN, interferon; SVR: sustained virological responder; R: relapse; NR: non-responder; RVR: rapid virological responder; EVR: early virological responder.

Acknowledgements

YM and KS were financially supported by the Ministry of Health, Labour and Welfare of Japan. They also received Grants-in-Aid for scientific research from the Ministry of Education, Culture, Sports, Science and Technology. MKwas financially supported by the 'Strategic Research-Based Support' Project for private universities; with matching funds from the Ministry of Education, Culture, Sports, Science and Technology.

Author details

[1]Center for Genomic Medicine, Kyoto University Graduate School of Medicine, 53 Shogoinkawahara-cho, Sakyo-ku, Kyoto 606-8507, Japan. [2]Department of Molecular Pathology, Tokyo Medical University, 6-1-1 Shinjuku, Shinjuku-ku, Tokyo 160-8402, Japan. [3]Department of Gastroenterology, Ogaki Municipal Hospital, 86-4 Minaminokawa-cho, Ogaki, Gifu 503-8502, Japan. [4]DNA Chip Research Inc., 43-1-1 Suehiro-cho, Tsurumi-ku, Yokohama, Kanagawa 230-0045, Japan. [5]Department of Molecular Life Science, Tokai University School of Medicine, 143 Shimokasuya, Isehara, Kanagawa 259-1193, Japan. [6]Research Institute, Chiba Institute for Technology, 2-17-1 Tsudanuma, Narashino, Chiba 275-0016, Japan.

Authors' contributions

YM and KS conceived and designed the experiments; YM, HT and KH performed the experiments; MT and MK performed statistical analysis; YM, MT, HT and AT contributed to writing and editing the manuscript. All authors read and approved the manuscript.

Competing interests

The authors declare that they have no competing interests.

Received: 13 June 2010 Accepted: 22 October 2010
Published: 22 October 2010

References

1. Guidotti LG, Chisari FV: **Immunobiology and pathogenesis of viral hepatitis.** *Annu Rev Pathol* 2006, 1:23-61.
2. Fried MW, Shiffman ML, Reddy KR, Smith C, Marinos G, Goncales FL, Haussinger D, Diago M, Carosi G, Dhumeaux D, Craxi A, Lin A, Hoffman J, Yu J: **Peginterferon alfa-2a plus ribavirin for chronic hepatitis C virus infection.** *N Engl J Med* 2002, **347(13)**:975-982.
3. Ambros V: **The functions of animal microRNAs.** *Nature* 2004, **431(7006)**:350-355.
4. Nilsen TW: **Mechanisms of microRNA-mediated gene regulation in animal cells.** *Trends Genet* 2007, **23(5)**:243-249.
5. Zamore PD, Haley B: **Ribo-gnome: the big world of small RNAs.** *Science (New York, NY)* 2005, **309(5740)**:1519-1524.
6. Pillai RS: **MicroRNA function: multiple mechanisms for a tiny RNA?** *RNA (New York, NY)* 2005, **11(12)**:1753-1761.
7. Lagos-Quintana M, Rauhut R, Yalcin A, Meyer J, Lendeckel W, Tuschl T: **Identification of tissue-specific microRNAs from mouse.** *Curr Biol* 2002, **12(9)**:735-739.

8. Sarasin-Filipowicz M, Krol J, Markiewicz I, Heim MH, Filipowicz W: **Decreased levels of microRNA miR-122 in individuals with hepatitis C responding poorly to interferon therapy.** *Nat Med* 2009, **15(1)**:31-33.
9. Ji J, Shi J, Budhu A, Yu Z, Forgues M, Roessler S, Ambs S, Chen Y, Meltzer PS, Croce CM, Qin LX, Man K, Lo CM, Lee J, Ng IO, Fan J, Tang ZY, Sun HC, Wang XW: **MicroRNA expression, survival, and response to interferon in liver cancer.** *N Engl J Med* 2009, **361(15)**:1437-1447.
10. Pedersen IM, Cheng G, Wieland S, Volinia S, Croce CM, Chisari FV, David M: **Interferon modulation of cellular microRNAs as an antiviral mechanism.** *Nature* 2007, **449(7164)**:919-922.
11. Jopling CL, Yi M, Lancaster AM, Lemon SM, Sarnow P: **Modulation of hepatitis C virus RNA abundance by a liver-specific MicroRNA.** *Science (New York, NY)* 2005, **309(5740)**:1577-1581.
12. Murakami Y, Aly HH, Tajima A, Inoue I, Shimotohno K: **Regulation of the hepatitis C virus genome replication by miR-199a(*).** *J Hepatol* 2009, **50(3)**:453-460.
13. Enomoto N, Sakuma I, Asahina Y, Kurosaki M, Murakami T, Yamamoto C, Ogura Y, Izumi N, Marumo F, Sato C: **Mutations in the nonstructural protein 5A gene and response to interferon in patients with chronic hepatitis C virus 1b infection.** *N Engl J Med* 1996, **334(2)**:77-81.
14. Akuta N, Suzuki F, Kawamura Y, Yatsuji H, Sezaki H, Suzuki Y, Hosaka T, Kobayashi M, Kobayashi M, Arase Y, Ikeda K, Miyakawa Y, Kumada H: **Prediction of response to pegylated interferon and ribavirin in hepatitis C by polymorphisms in the viral core protein and very early dynamics of viremia.** *Intervirology* 2007, **50(5)**:361-368.
15. Asselah T, Bieche I, Narguet S, Sabbagh A, Laurendeau I, Ripault MP, Boyer N, Martinot-Peignoux M, Valla D, Vidaud M, Marcellin P: **Liver gene expression signature to predict response to pegylated interferon plus ribavirin combination therapy in patients with chronic hepatitis C.** *Gut* 2008, **57(4)**:516-524.
16. Feld JJ, Nanda S, Huang Y, Chen W, Cam M, Pusek SN, Schweigler LM, Theodore D, Zacks SL, Liang TJ, Fried MW: **Hepatic gene expression during treatment with peginterferon and ribavirin: Identifying molecular pathways for treatment response.** *Hepatology* 2007, **46(5)**:1548-1563.
17. Chen L, Borozan I, Feld J, Sun J, Tannis LL, Coltescu C, Heathcote J, Edwards AM, McGilvray ID: **Hepatic gene expression discriminates responders and nonresponders in treatment of chronic hepatitis C viral infection.** *Gastroenterology* 2005, **128(5)**:1437-1444.
18. Tanaka Y, Nishida N, Sugiyama M, Kurosaki M, Matsuura K, Sakamoto N, Nakagawa M, Korenaga M, Hino K, Hige S, Ito Y, Mita E, Tanaka E, Mochida S, Murawaki Y, Honda M, Sakai A, Hiasa Y, Nishiguchi S, Koike A, Sakaida I, Imamura M, Ito K, Yano K, Masaki N, Sugauchi F, Izumi N, Tokunaga K, Mizokami M: **Genome-wide association of IL28B with response to pegylated interferon-alpha and ribavirin therapy for chronic hepatitis C.** *Nature genetics* 2009, **41(10)**:1105-1109.
19. Younossi ZM, Baranova A, Afendy A, Collantes R, Stepanova M, Manyam G, Bakshi A, Sigua CL, Chan JP, Iverson AA, Santini CD, Chang SY: **Early gene expression profiles of patients with chronic hepatitis C treated with pegylated interferon-alfa and ribavirin.** *Hepatology* 2009, **49(3)**:763-774.
20. Dudoit S, Fridlyand J: **A prediction-based resampling method for estimating the number of clusters in a dataset.** *Genome Biol* 2002, **3(7)**: RESEARCH0036.
21. Dudoit S, Fridlyand J: **Bagging to improve the accuracy of a clustering procedure.** *Bioinformatics* 2003, **19(9)**:1090-1099.
22. **National Institutes of Health Consensus Development Conference Statement: Management of hepatitis C: 2002–June 10-12, 2002.** *Hepatology* 2002, **36(5 Suppl 1)**:S3-20.
23. Ferenci P, Fried MW, Shiffman ML, Smith CI, Marinos G, Goncales FL, Haussinger D, Diago M, Carosi G, Dhumeaux D, Craxi A, Chaneac M, Reddy KR: **Predicting sustained virological responses in chronic hepatitis C patients treated with peginterferon alfa-2a (40 KD)/ribavirin.** *J Hepatol* 2005, **43(3)**:425-433.
24. Sonkoly E, Stahle M, Pivarcsi A: **MicroRNAs and immunity: novel players in the regulation of normal immune function and inflammation.** *Seminars in cancer biology* 2008, **18(2)**:131-140.
25. Lindsay MA: **microRNAs and the immune response.** *Trends in immunology* 2008, **29(7)**:343-351.
26. Chen PY, Manninga H, Slanchev K, Chien M, Russo JJ, Ju J, Sheridan R, John B, Marks DS, Gaidatzis D, Sander C, Zavolan M, Tuschl T: **The developmental miRNA profiles of zebrafish as determined by small RNA cloning.** *Genes & development* 2005, **19(11)**:1288-1293.
27. Peng X, Li Y, Walters KA, Rosenzweig ER, Lederer SL, Aicher LD, Proll S, Katze MG: **Computational identification of hepatitis C virus associated microRNA-mRNA regulatory modules in human livers.** *BMC Genomics* 2009, **10**:373.
28. Gong AY, Zhou R, Hu G, Li X, Splinter PL, O'Hara SP, LaRusso NF, Soukup GA, Dong H, Chen XM: **MicroRNA-513 regulates B7-H1 translation and is involved in IFN-gamma-induced B7-H1 expression in cholangiocytes.** *J Immunol* 2009, **182(3)**:1325-1333.
29. Yu D, Rao S, Tsai LM, Lee SK, He Y, Sutcliffe EL, Srivastava M, Linterman M, Zheng L, Simpson N, Ellyard JI, Parish IA, Ma CS, Li QJ, Parish CR, Mackay CR, Vinuesa CG: **The transcriptional repressor Bcl-6 directs T follicular helper cell lineage commitment.** *Immunity* 2009, **31(3)**:457-468.
30. Hsu PW, Lin LZ, Hsu SD, Hsu JB, Huang HD: **ViTa: prediction of host microRNAs targets on viruses.** *Nucleic acids research* 2007, **35(Database issue)**:D381-385.
31. Pulendran B, Tang H, Denning TL: **Division of labor, plasticity, and crosstalk between dendritic cell subsets.** *Curr Opin Immunol* 2008, **20(1)**:61-67.
32. Wertheimer AM, Bakke A, Rosen HR: **Direct enumeration and functional assessment of circulating dendritic cells in patients with liver disease.** *Hepatology* 2004, **40(2)**:335-345.
33. Dienstag JL, McHutchison JG: **American Gastroenterological Association technical review on the management of hepatitis C.** *Gastroenterology* 2006, **130(1)**:231-264.

Pre-publication history
The pre-publication history for this paper can be accessed here:
http://www.biomedcentral.com/1755-8794/3/48/prepub

doi:10.1186/1755-8794-3-48
Cite this article as: Murakami *et al.*: Hepatic microRNA expression is associated with the response to interferon treatment of chronic hepatitis C. *BMC Medical Genomics* 2010 **3**:48.

Polyubiquitin conjugation to NEMO by triparite motif protein 23 (TRIM23) is critical in antiviral defense

Kei-ichiro Arimoto[a,b], Kenji Funami[c], Yasushi Saeki[d], Keiji Tanaka[d], Katsuya Okawa[e], Osamu Takeuchi[f], Shizuo Akira[f], Yoshiki Murakami[b], and Kunitada Shimotohno[c,1]

[a]Laboratory of Biological Protection, Institute for Virus Research, Graduate School of Medicine, Kyoto University, Shogo-in, Sakyo-ku, Kyoto 606-8507, Japan; [c]Research Institute, Chiba Institute of Technology, 2-17-1, Tsudanuma, Narashino City, Chiba 275-0016, Japan; [d]Laboratory of Frontier Science, Core Technology and Research Center, Tokyo Metropolitan Institute of Medical Science, 2-1-6, Kamikitazawa, Setagaya-ku, Tokyo 156-8506, Japan; [e]Kyowa Hakko Kirin Co., Ltd., Takasaki City, Sunto-gun, Shizuoka 411-8731, Japan; [f]Laboratory of Host Defense, World Premier International Immunology Frontier Research Center, Research Institute for Microbial Diseases, Osaka University, 3-1 Yamada-oka, Suita, Osaka 565-0871, Japan; and [b]Center for Genomic Medicine, Kyoto University, Shogo-in, Sakyo-ku, Kyoto 606-8507, Japan

Edited by Diane E. Griffin, Johns Hopkins Bloomberg School of Public Health, Baltimore, MD, and approved July 16, 2010 (received for review April 8, 2010)

The rapid induction of type I IFN is a central event of the innate defense against viral infections and is tightly regulated by a number of cellular molecules. Viral components induce strong type I IFN responses through the activation of toll-like receptors (TLRs) and intracellular cytoplasmic receptors such as an RNA helicase RIG-I and/or MDA5. According to recent studies, the NF-κB essential modulator (NEMO, also called IKKγ) is crucial for this virus-induced antiviral response. However, the precise roles of signal activation by NEMO adaptor have not been elucidated. Here, we show that virus-induced IRF3 and NF-κB activation depends on the K(lys)-27-linked polyubiquitination to NEMO by the novel ubiquitin E3 ligase triparite motif protein 23 (TRIM23). Virus-induced IRF3 and NF-κB activation, as well as K27-linked NEMO polyubiquitination, were abrogated in TRIM23 knockdown cells, whereas TRIM23 knockdown had no effect on TNFα-mediated NF-κB activation. Furthermore, in NEMO-deficient mouse embryo fibroblast cells, IFN-stimulated response element-driven reporter activity was restored by ectopic expression of WT NEMO, as expected, but only partial recovery by NEMO K165/309/325/326/344R multipoints mutant on which TRIM23-mediated ubiquitin conjugation was substantially reduced. Thus, we conclude that TRIM23-mediated ubiquitin conjugation to NEMO is essential for TLR3- and RIG-I/MDA5-mediated antiviral innate and inflammatory responses.

innate immunity | signal transduction | virus infection

Upon viral infection, host cells recognize the viral components and activate innate immune signaling to exert antiviral responses (1–4). RIG-I and/or MDA5 sense viral dsRNA (5–8) and are recruited to another antiviral signaling adaptor, IPS-1 (also called MAVS, Cardif, or VISA) (9–12). IPS-1 directly interacts with TRAF3 and triggers auto-ubiquitination of TRAF3, which then activates TBK1 and IKKε, leading to activation of transcription factors NF-κB and IRF3 (13, 14). A recent study indicated that NEMO acts upstream of TBK1 and IKKε and is essential for virus-induced TLR3- and RIG-I/MDA5–mediated antiviral activation (15).

Because rapid induction of type I IFN expression is the key process in initiating the innate antiviral response, clarification of NEMO-mediated antiviral signaling is important for understanding innate immune signaling; however, NEMO-mediated antiviral signaling is not well elucidated. Recent studies indicate that several ubiquitin E3 ligases are involved in the regulation of innate immune signaling (16–21). We identified the ubiquitin E3 ligase TRIM23 (Triparite motif protein 23), also named ADP ribosylation factor domain protein 1 (ARD1), which was reported to have E3 ligase activity in vitro (22), that functioned as an E3 ligase for NEMO ubiquitin conjugation. TRIM23 exerts a potent antiviral state following its overexpression. Furthermore, we demonstrated that antiviral activity depends not on K(Lys)63-linked but on K27-linked polyubiquitin conjugation to multiple sites of NEMO by TRIM23 expression. Virus-induced IRF3 and NF-κB activation, as well as K27-linked NEMO polyubiquitination, were abrogated in TRIM23 knockdown cells (including primary mouse embryonic fibroblasts), whereas TRIM23 knockdown had no effect on TNFα-mediated NF-κB activation.

Results

TRIM23 Interacts with NEMO. Recent studies indicate that several ubiquitin E3 ligases are involved in the regulation of innate immune signaling (16–21). We previously reported that the E3 ubiquitin ligase RNF125 negatively regulates RIG-I signaling (17), and it has been reported that RNF125 is also a T-cell activator (23), which suggests the presence of plural functions of RNF125 in regulation of cell proliferation. To identify genes affected by RNF125, we conducted microarray analysis (mock- vs. RNF125-transfected 293T cells) and found the gene for TRIM23 up-regulated ~3-fold (Fig. S1*A*). Through analysis of function of TRIM23, we also found that TRIM23 up-regulated the NF-κB–driven reporter gene in cells expressing NEMO. Introduction of TRIM23 slightly activated NF-κB in cells expressing endogenous NEMO and substantially activated NF-κB in cells ectopically expressing NEMO. Furthermore, we found that NEMO migrated slowly by SDS/PAGE when coexpressed with TRIM23 (Fig. S1*B*), suggesting posttranslational modification, most likely ubiquitin conjugation by TRIM23. It has been reported that TRIM23 has E3 ligase activity in vitro (22). Because ubiquitin E3 ligases generally require association with the substrate to execute its enzyme activity, we analyzed the association of TRIM23 with NEMO by GST-pulldown and coimmunoprecipitation assays. These results showed that TRIM23 interacted with NEMO directly (Fig. S1*C*). Deletion analysis of NEMO showed that both the CC1 and LZ domains of NEMO are essential for this interaction (Fig. 1 *A* and *C*). Binding analysis showed further that the TRIM23 C-terminal ARF domain interacted with NEMO CC1 and LZ domains as effectively as the full-length TRIM23, whereas the RING finger and B-box/B-box/CCD domains did not (Fig. 1 *A*, *B*, and *D*). Bifluorescent complementation analysis also revealed interaction of NEMO with TRIM23 in living HeLa cells (Fig. 1*E*). An interaction between endogenous NEMO and TRIM23 was also detected in 293T cells (Fig. 1*F*).

TRIM23 Is an E3 Ligase for Conjugation of K27 Type Ubiquitin to NEMO. To examine whether TRIM23 ubiquitinates NEMO, NEMO-FLAG was coexpressed with WT TRIM23 or its E3 ligase activity-defective RING mutants (TRIM23C34A and TRIM23ΔRING). Although TRIM23 expression markedly increased the ubiquitin conjugation levels of NEMO-FLAG, neither TRIM23C34A nor TRIM23ΔRING had any effect (Fig. 2*A*). Levels of ubiquitin conjugation to NEMO were enhanced by increasing amounts of TRIM23. Under these conditions, the mRNA levels of NEMO, GAPDH, and tubulin were unchanged (Fig. 2*B*). By analyzing mutants of ubiquitin for conjugation to NEMO in a TRIM23-dependent manner, we observed that the K27-only type could be

Author contributions: K.-i.A., K.F., and K.S. designed research; K.-i.A. performed research; O.T., S.A., and Y.M. contributed new reagents/analytic tools; K.-i.A., K.F., Y.S., K.T., K.O., O.T., S.A., Y.M., and K.S. analyzed data; and K.-i.A. and K.S. wrote the paper.

The authors declare no conflict of interest.

This article is a PNAS Direct Submission.

[1]To whom correspondence should be addressed. E-mail: kunitada.shimotono@it-chiba.ac.jp.

This article contains supporting information online at www.pnas.org/lookup/suppl/doi:10.1073/pnas.1004621107/-/DCSupplemental.

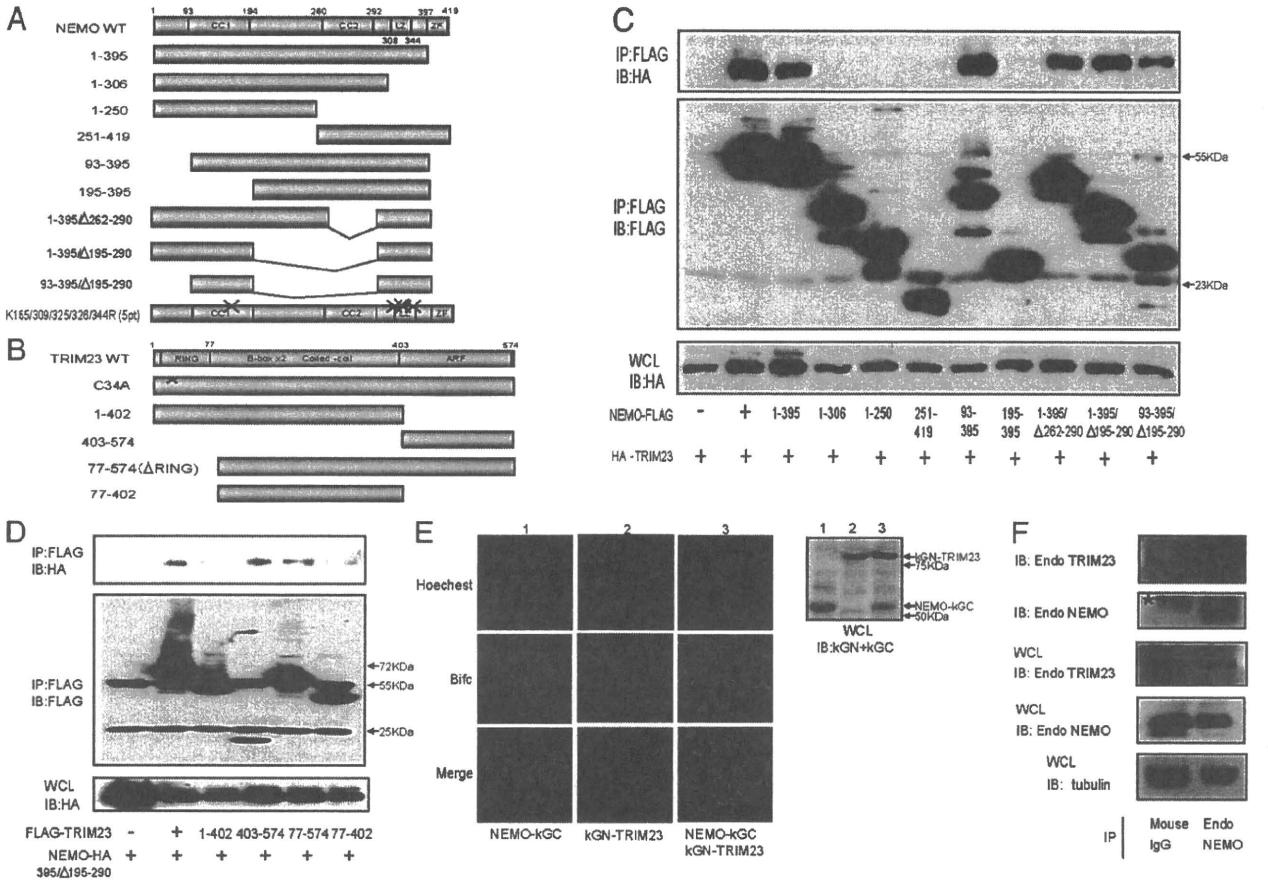

Fig. 1. Interaction between NEMO and TRIM23. (*A* and *B*) Schematic drawings of NEMO, TRIM23, and their derivatives used in this work. CC1 coiled-coil domain 1; CC2, coiled-coil domain 2; LZ, leucine zipper; ZF, zinc finger. RING finger domain, B-box-B-box/CCD (coiled-coil domain), and ARF (ADP ribosylation factor) domain in TRIM23 are shown. X indicates sites of mutagenesis described in the text. (*C*) 293T cells were cotransfected with plasmids encoding HA-TRIM23 and NEMO-FLAG or its mutants. (*D*) NEMO CC1 and LZ domains interacted with the TRIM23 ARF region in 293T cells. (*E*) HeLa cells were transfected with plasmids encoding NEMO-kGC and kGN-Mock, kGN-TRIM23 and Mock-kGC, or NEMO-kGC and kGN-TRIM23. Nuclear localizations were detected by Hoechst 33342. Bifc signal revealed TRIM23-NEMO–specific association. Expression of NEMO and TRIM23 in HeLa cells were also confirmed by immunoblot using anti-kGN and -KGC antibody. (*F*) Interaction of endogenous NEMO with endogenous TRIM23 in 293T cells 24 h after SV infection. Asterisk denotes nonspecific band.

conjugated as polyubiquitin to NEMO (Fig. 2*C*). This was further confirmed by the ubiquitin conjugation of K63R, but not of K27R mutant of ubiquitin (Fig. 2*D*). NF-κB reporter activity in cells ectopically expressing K27-only ubiquitin was higher when compared with K27R ubiquitin in NEMO and TRIM23 expressing 293T cells (Fig. 2*E*). An in vitro ubiquitination assay showed that TRIM23 could use UbcH1, 5a, 5b, 5c, and 13/Mms2 as an ubiquitin E2-conjugating enzyme (Fig. S2*A*). Among these E2 enzymes, the presence of UbcH5s could conjugate ubiquitin to NEMO at shorter time of reaction, suggesting that the presence of UbcH5s, rather than UbcH1 or Ubc13/Mms2, may have a strong ability to conjugate ubiquitin to NEMO. When using the K27-only ubiquitin mutant, only UbcH5a, 5b, and 5c showed ubiquitin conjugation activity, suggesting that these may be the major E2 enzymes functioning in vivo (Fig. S2*B*).

In the analysis using deletion mutants of NEMO, it was observed that TRIM23 could conjugate ubiquitin preferentially to the NEMO CC1 and LZ domains (Fig. S3*A*). Single point mutation of K to R in these domains of WT-NEMO was not affected by TRIM23 expression at the ubiquitin conjugation level (Fig. S3*B*). In an analysis of several NEMO mutants having mutations on plural lysine residues in these domains of NEMO, we observed that ubiquitin conjugation to NEMO K165/309/325/326/344R, NEMO-5pt, was substantially reduced when compared with that of the WT NEMO. This suggests the importance of these five lysine residues in TRIM23-dependent ubiquitin conjugation to NEMO, at least in part (Fig. 2*F*).

TRIM23 Exerts a Potent Antiviral State Following Its Overexpression. NEMO has critical roles in virus-induced innate and inflammatory responses (15). To investigate the roles of TRIM23-mediated NEMO ubiquitination, we examined IFNβ, ISRE, or NF-κB promoter-driven reporter activity by expressing TRIM23 or TRIM23C34A after treating cells with poly I:C, infection with Sendai virus (SV), or coexpressing upstream adaptor molecules of innate immunity signaling. Ectopic expression of WT TRIM23, together with plasmids encoding TLR3, RIG-I, or IPS1, upregulated ISRE reporter activity. Expression of TRIM23C34A suppressed the reporter activity (Fig. S4A). Same results were observed in both IFNβ and NF-κB reporter assays with polyI:C or SV infection (Fig. S4 *B* and *C*). Consistent with the NEMO ubiquitination level (Fig. 2*B*), NF-κB promoter activity considerably increased and decreased dose-dependently with TRIM23 and TRIM23C34A expression, respectively (Fig. S4*D*). Reduction of the reporter activity by TRIM23C34A seems to have a dominant negative effect on endogenous TRIM23, although the precise mechanism requires further clarification.

Suppression of TRIM23 Impaired K27-Linked Ubiquitin Conjugation to NEMO and Virus-Induced Antiviral Activity. To examine the physiological roles of TRIM23 in antiviral innate immunity, we analyzed IFNβ and NF-κB reporter activity in cells knocked-down of TRIM23 by specific siRNA. We also established 293T cells that were knocked down TRIM23 constitutively (Fig. 3*A*). TRIM23 knockdown impaired IFNβ reporter activity by SV infection and

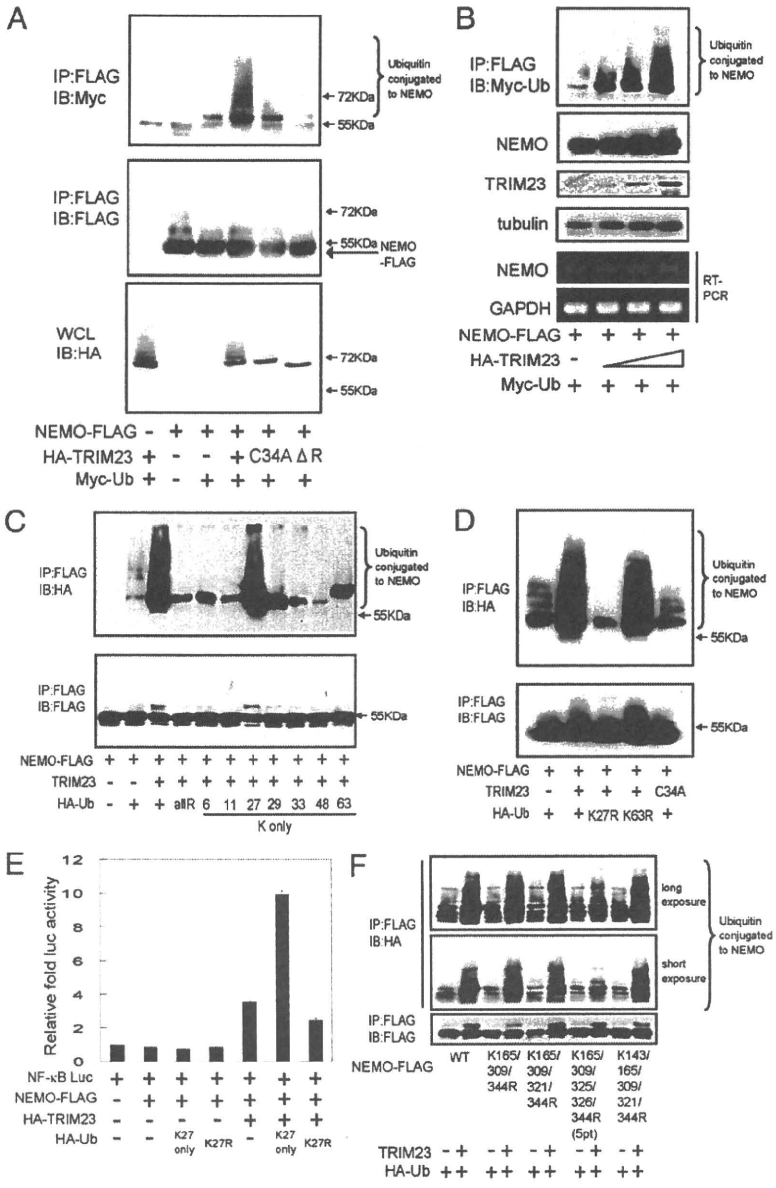

Fig. 2. TRIM23 conjugates K27-linked polyubiquitin to NEMO at multiple sites. (*A*) 293T cells were cotransfected with plasmids encoding NEMO-FLAG, HA-TRIM23, HA-TRIM23C34A (abbreviated as C34A), HA-TRIM23 ΔRING (abbreviated as ΔR), and Myc-Ub as indicated. (*B*) Ubiquitin conjugation to NEMO is enhanced dose-dependent TRIM23 expression. 293T cells were cotransfected with plasmids encoding NEMO-FLAG, Myc-Ub, or plasmid (0–2 μg) expressing HA-TRIM23. Levels of NEMO and GAPDH mRNA are also shown. (*C*) 293T cells were cotransfected with plasmids expressing NEMO-FLAG, TRIM23, and HA-Ub (WT, KallR, K6-, 11-, 27-, 29-, 33-, 48-, and 63-only). (*D*) 293T cells were cotransfected with plasmids encoding NEMO-FLAG, TRIM23, TRIM23C34A, and HA-Ub (WT, K27R, or K63R). (*E*) The K27-only ubiquitin conjugation enhanced NEMO-TRIM23-mediated NF-κB reporter activity. 293T cells were transfected with plasmids encoding NF-κB-luc, NEMO-FLAG, or HA-TRIM23, together with plasmids expressing HA-K27-only Ub or HA-K27R Ub as indicated. (*F*) NEMO KR mutants expressing in 293T cells transfected with plasmids encoding TRIM23 and HA-Ub were analyzed for their ubiquitin conjugation.

poly I:C treatment, depending on the knockdown level of TRIM23 (Fig. 3*A*). Similar results were obtained in the murine leukemic monocyte macrophage cell line Raw264.7 (Fig. S4*E*). TRIM23 knockdown also impaired NF-κB reporter activity in poly I:C treatment, but did not impair that which was activated by TNFα treatment (Fig. 3*A*). Virus-induced IFNβ mRNA and phosphorylation of STAT1 and IRF3, as well as IFN-inducible ISG15, were substantially reduced in cells expressing sh-TRIM23-1 (Fig. 3*B*). Thus, quantitative analysis indicated that the TRIM23 level was correlated with antiviral inflammatory and IFN responses (Fig. 3*A* and *B*). TRIM23 knockdown also impaired IFNβ reporter activity activated by RIG-I and IPS-1 expression in 293T cells (Fig. 3*C*). NEMO is upstream of TBK1 (15). To investigate whether TBK1-triggered IFNβ activation is regulated by TRIM23 expression, we conducted an IFNβ luciferase reporter assay using NEMO$^{-/-}$ MEFs. As a result, TBK1-mediated IFNβ up-regulation was not affected at all in TRIM23 siRNA-treated cells (Fig. 3*D*).

Furthermore, upon SV infection, we did not observe TRIM23-mediated ISRE reporter enhancement in TBK1/IKKi double knockout MEFs (TBK1$^{-/-}$IKKi$^{-/-}$), although the activity was significantly enhanced in WT MEFs (Fig. S4*F*). These results indicate that the TRIM23-NEMO complex is important for antiviral responses, and that TRIM23 does not exert its function directly on downstream molecules of NEMO, such as TBK1, in antiviral signaling.

IRF3 dimerization and IRF3 phosphorylation promoted by IPS-1 expression or SV infection were impaired in TRIM23 knockdown 293T cells (Fig. 3*E*). In 293T cells, the effect of knockdown of TRIM23 was more clearly observed than the effect of overexpression of TRIM23, suggesting that endogenous TRIM23 in 293T cells was high and can sufficiently function at physiological levels for antiviral responses in this cell line.

To further examine the physiological relevance of TRIM23 in antiviral responses, we measured the amount of IFNβ in culture medium by ELISA using primary WT and TRAF6$^{-/-}$ MEFs. TRIM23 knockdown decreased IFNβ production with SV infection in both cells (Fig. 3*F*). The level of phosphorylated STAT1 was up-regulated by the ectopic expression of TRIM23, and down-regulated by the expression of TRIM23C34A in WT as well as TRAF6$^{-/-}$MEFs (Fig. S5*A*). These results suggest that TRIM23 is more important than TRAF6 for virus-induced IFNβ production, which is in line with works reported by other groups (24–26). Importantly, we observed that SV-induced endogenous NEMO ubiquitination diminished in TRIM23 knockdown 293T cells (Fig.

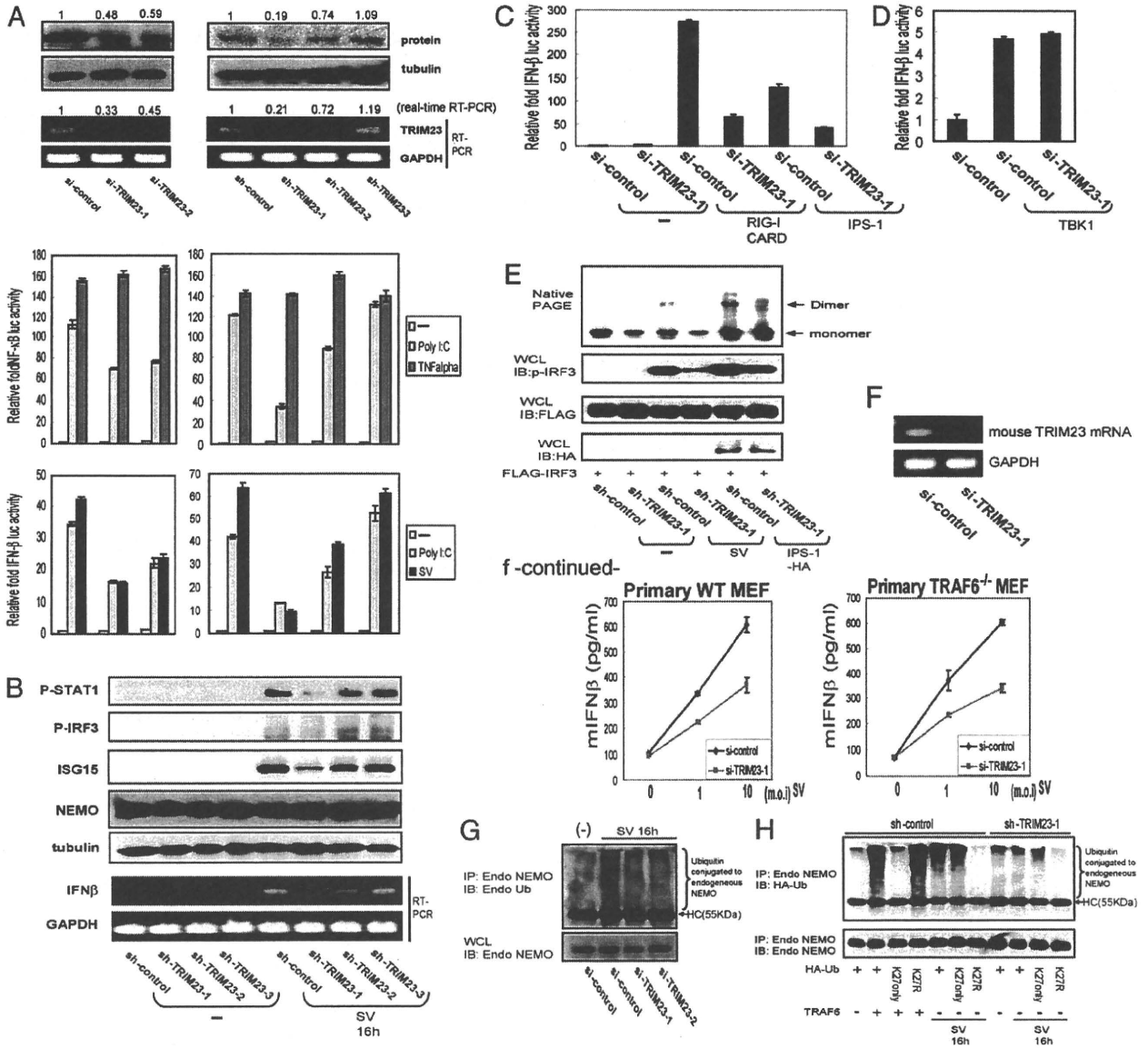

Fig. 3. TRIM23 knockdown impaired both ubiquitin conjugation to NEMO and antiviral responses. (*A*) Efficiency of TRIM23 knockdown using siRNA and shRNA in 293T cells (*Top*). Si-TRIM23-1 and sh-TRIM23-1 significantly suppressed levels of TRIM23. Protein and mRNA levels of TRIM23 were also quantified by ImageJ software and real-time RT-PCR, respectively (*Top*). The mRNA levels of TRIM23 were also visualized by RT-PCR (*Top*). Under these conditions, NF-κB (*Middle*) and IFNβ (*Bottom*) luciferase activities were measured after treatment with Poly I:C (20 μg/mL), TNFα (10 ng/mL), or infected with SV (m.o.i. 10). (*B*) Control and TRIM23 knockdown 293T cells were infected with or without SV (m.o.i 10) for 16 h. Cell lysates were subject to Western blot with the indicated antibodies. The levels of IFNβ and GAPDH mRNA were also analyzed. (*C*) 293T cells were treated with si-TRIM23-1 or control si-RNA. At 48 h after siRNA transfection, cells were further transfected with plasmids encoding IFNβ-Luc, RIG-I CARD, or IPS-1. At 72 h after siRNA transfection, luciferase activity was measured. (*D*) NEMO$^{-/-}$ MEFs were treated with si-TRIM23-1 or control si-RNA. At 48 h after siRNA transfection, cells were further transfected with plasmids encoding IFNβ-Luc and TBK1. At 72 h after siRNA transfection, luciferase activity was measured. (*E*) 293T cells treated with sh-TRIM23-1 were transfected with plasmids encoding FLAG-IRF3 or IPS-1-HA, and then cells were mock infected or infected with SV for 16 h as indicated. Dimer formation of IRF3 was analyzed. Phosphorylated IRF3 and the total amount of IRF3 in cell lysates as well as IPS-1-HA are also shown. (*F*) Suppression of IFNβ production in WT and TRAF6$^{-/-}$ MEFs treated with si-TRIM23-1. The mRNA levels of murine TRIM23 were visualized by RT-PCR (*Upper*). IFNβ in culture medium was analyzed by ELISA (*Lower*). (*G*) 293T cells were treated with control siRNA, si-TRIM23-1, or si-TRIM23-2. At 48 h after the transfection, cells were mock infected or infected with SV (m.o.i. 10). At 16 h after infection, cell lysates were analyzed for ubiquitin conjugation of NEMO. (*H*) TRAF6 did not enhance K27-linked ubiquitin conjugation to NEMO, but SV infection did. However, this conjugation was abrogated by TRIM23 knockdown. The sh-control and sh-TRIM23-1–treated cells were transfected with plasmids encoding HA-Ub WT, K27-only, or K27R. Cells were then either transfected with plasmids encoding TRAF6 or infected with SV for 16 h.

3*G*). Ubiquitin conjugation to endogenous NEMO occurred in K27-only type after SV infection, which was reduced in TRIM23 knockdown 293T cells. In contrast, the ectopic expression of TRAF6 enhanced K27R and not the K27-only type (Fig. 3*H*). Endogenous ubiquitin conjugation to endogenous NEMO was up-regulated upon viral infection, and TRIM23 knockdown impaired this. Nonetheless, the protein level of TRIM23 and the interaction between TRIM23 and NEMO were not affected by viral infection (Fig. S5*B*). Considering that some E2 ubiquitin conjugating enzymes are IFN inducible and that several E2 enzymes and E4 enzymes affect ubiquitin assembly (27–30), it may be that TRIM23-mediated ubiquitin conjugation to NEMO is regulated

by a specific E2 (such as UbcH5, as suggested in an in vitro assay in this study) and/or E4 enzyme(s) that respond to viral infection. Indeed, in a preliminary experiment, the association of NEMO and UbcH5 was increased by Sendai virus infection (Fig. S5*B*). Furthermore, knockdown of UbcH5 not UbcH1 or Ubc13 substantially impaired TRIM23-mediated ubiquitin conjugation to NEMO (Fig.S5*C*). Moreover, TRIM23 conjugates UbcH5s slightly stronger than UbcH1 or Ubc13 in 293T cells (Fig.S5*D*).

To investigate whether TRIM23-mediated NEMO polyubiquitination influences antiviral responses, we measured ISRE and NF-κB luciferase reporter activity in NEMO$^{-/-}$ MEFs transiently expressing WT-NEMO, NEMO-5pt, or vector alone. The efficiency of transfection was the same as judged from Western blots of NEMO (Figs. 4 *A* and *B*). After SV infection, both ISRE and NF-κB luciferase activities in cells expressing NEMO-5pt deteriorated when compared with WT-NEMO expression (Figs. 4 *A* and *B, Left*). Ubiquitin conjugation to NEMO-5pt by TRIM23 was reduced when compared with WT-NEMO (Figs. 2*F* and 4*C*). Despite a significant reduction in its level of ubiquitination, NEMO-5pt interacted with TRIM23 (Fig. S6) as efficiently as WT-NEMO, suggesting that the reduction of activation of downstream reporter genes by NEMO-5pt was attributed to a lower level of ubiquitin conjugation. In contrast, NF-κB luciferase activity in cells expressing WT-NEMO and NEMO-5pt by ectopic expression of TRAF6 in NEMO$^{-/-}$ MEFs did not show significant difference (Fig. 4*B, Right*). Ubiquitin conjugation to WT-NEMO and NEMO-5pt in cells expressing TRAF6 was almost the same level (Fig. 4*C*). Ectopic expression of TRIM23 alone or the expression of the deletion mutant of NEMO, which cannot interact with TRIM23 and therefore lack ubiquitin conjugation, in NEMO$^{-/-}$ MEFs did not activate ISRE- and NF-κB reporter genes upon SV infection (Fig. S7). Thus, it is likely that ubiquitin conjugation to NEMO by TRIM23 is a requisite for the activation of ISRE- and NF-κB reporter genes in SV infection.

TRIM23 Knockdown Cells Produce More Virus. To corroborate that TRIM23 is involved in virus-mediated innate signaling, we infected vesicular stomatitis virus (VSV) at various multiplicity of infection (m.o.i.) to WT and TRIM23 knockdown primary MEF cells. Silencing of endogenous TRIM23 resulted in higher number of cells killed compared with the control cells (Fig. 4*D, Left*). Quantification of virus titration showed that the yield of infectious virus in TRIM23 knockdown cells was ~1 log higher than that in WT MEF cells (Fig. 4*D, Right*). Similar results were obtained in 293T cells, in which experiment the effect of IPS1 expression was also shown (Fig. S8). Thus, we conclude that TRIM23 plays important roles in facilitating TLR3- and RIG-I/MDA5-mediated antiviral innate signaling.

Discussion

Here, we demonstrated an essential function of TRIM23 in antiviral activity. TRIM23 induces K27-linked polyubiquitination of NEMO, leading to the activation of downstream signaling for antiviral function. Virus-induced production of endogenous IFN and IFN-inducible gene expression, as well as K27-linked NEMO polyubiquitination, were substantially impaired by TRIM23 knockdown, which was not limited to cultured cell lines but was also seen in primary WT and TRAF6$^{-/-}$ MEFs. These results clearly indicate that TRIM23 plays important roles in antiviral signaling in physiologically immunocompetent cells.

Upon viral infection, TRAF3 auto-ubiquitination is required for IRF3 activation, but there is no direct evidence that TRAF3 conjugates ubiquitin to NEMO. In this study, we showed that TRIM23 directly interacted with NEMO and conjugated ubiquitin to it. On the other hand, we also observed interaction between TRAF3 and TRIM23 in coimmunoprecipitation assays (Fig. S9*A*). For this reason, we speculate that TRIM23 sits between TRAF3 and NEMO (Fig. S9*B*). However, how TRAF3 transmits antiviral signals to the TRIM23-NEMO complex should be examined in the future.

We showed that TRIM23-mediated conjugation of K27-type uniquitin to NEMO in 293T cells occurred as efficient as the conjugation of WT ubiquitin (Fig. 2*C*). Furthermore, we showed that ubiquitin conjugation to endogenous NEMO was higher in cells ectopically expressing K27-only ubiquitin than in cells

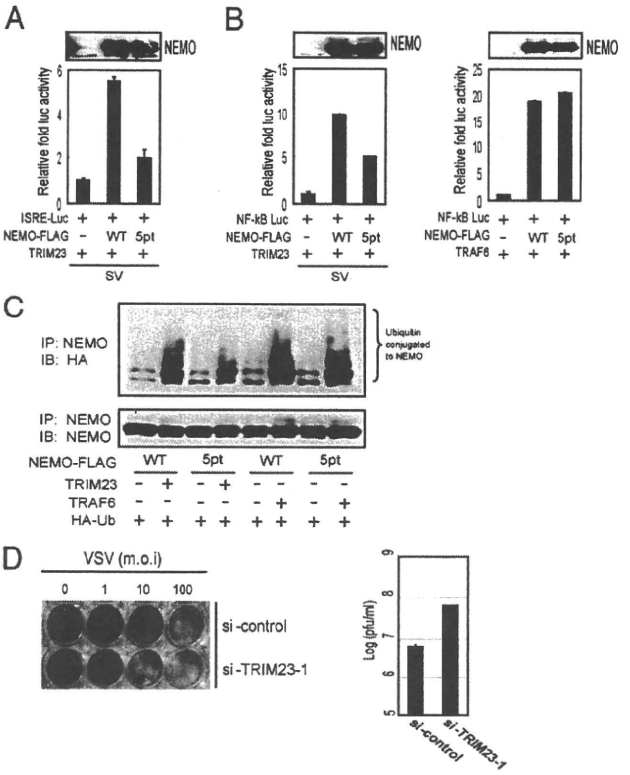

Fig. 4. Ubiquitin conjugation to NEMO by TRIM23 affects host defense. (*A*) NEMO$^{-/-}$ MEFs were transfected with plasmids encoding ISRE-Luc, TRIM23, and WT-NEMO or NEMO-5pt. At 8 h after transfection, cells were infected with SV for 16 h. (*B*) NEMO$^{-/-}$ MEFs were transfected with plasmids encoding NF-κB–Luc, TRIM23, and WT-NEMO or NEMO-5pt. At 8 h after transfection, cells were treated with SV for 16 h (*Left*). NEMO$^{-/-}$ MEFs were transfected with plasmids encoding NF-κB-Luc, TRAF6, and WT-NEMO or NEMO-5pt (*Right*). Cells were harvested 24 h after transfection, and luciferase activity was measured. The amount of NEMO in cell lysates, as an indicator of transfection efficiency, was measured. (*A* and *B*). (*C*) 293T cells were transfected with plasmids encoding TRIM23, TRAF6, FLAG-NEMO, or NEMO-5pt as indicated. (*D*) TRIM23 knockdown primary MEF cells allow virus production at a higher level than control cells. The primary MEFs were treated with control si-RNA or si-TRIM23-1 as indicated. At 60 h after transfection, VSV was infected with m.o.i. as indicated. Cells were stained at 24 h after infection (*Left*). Data are representative of two experiments. At 12 h after infection, virus titer was measured according to $TCID_{50}$ protocol (*Right*). Data are mean ± SD ($P < 0.001$, Student's *t* test, $n = 3$).

expressing K27R ubiquitin upon viral infection (Fig. 3*H*). Moreover, TRIM23 could conjugate K27-only ubiquitin to NEMO in vitro using UbcH5s as E2 enzyme (Fig. S2*B*). Importantly, knockdown of UbcH5s suppressed ubiquitin conjugation of NEMO in vivo, but knockdown of UbcH1 and Ubc13 did not (Fig. S5*C*), which may support an important role of UbcH5s in vivo. However, this does not discriminate against the possibility that other E2 enzymes also are involved in ubiquitin conjugation to NEMO in a concerted manner. Although it is strongly suggested that TRIM23 conjugates K27-type ubiquitin to NEMO, it remains further to analyze whether TRIM23 alone or TRIM23 together with other factor(s) exerts selecting activity of K27-type ubiquitin conjugation to NEMO. Recently, K63 type of ubiquitin was shown to be conjugated to NEMO upon VSV infection by in vitro ubiquitin conjugation analysis (31). However, this paper did not show the data that indicate lack of K63 ubiquitin conjugation in the lysate derived from uninfected cells. Thus, it is not clear whether K63 type ubiquitin conjugation to NEMO by VSV infection reflects physiological relevance.

There are several different ubiquitin modifications to NEMO to exert NF-κB regulation, Lys(K)-63–linked NEMO ubiquitination by several cellular events for NF-κB activation (32–35), and

LUBAC-mediated linear ubiquitin conjugation to NEMO in TNFα-mediated NF-κB activation in Ubc13-independent manner (36). Moreover, recently, it was reported that bacterial E3 ligase IpaH9.8 promotes K27-linked ubiquitin conjugation to NEMO and facilitates degradation of NEMO with unidentified molecule(s) activated by NOD1 signaling (37). Although both E3 ligases, TRIM23, and bacterially encoded IpaH9.8 conjugate K27-linked ubiquitin to NEMO, the outcomes are totally different. Because these ligases conjugate K27-linked ubiquitin to different lysine residues of NEMO, it is suggested that K27 ubiquitin conjugation exerts variety roles to NEMO with yet unclarified mechanisms.

We conducted microarray analysis as a primary tool for searching E3 ligases involved in innate immunity. Up-regulation of TRIM23 by ectopic expression of RNF125 in 293T cells suggests the presence of mutual interaction in expression of these genes. Moreover, these proteins may cooperatively function to antiviral signaling, although precise functional interaction between these proteins is not clear.

Additional works, including analysis of TRIM23-deficient mice, may reveal the specific role(s) of TRIM23 in the innate immune response to viral infection. As many viruses have evolved tactics to escape host immunity, it is likely that some viruses may target TRIM23 to establish successful infection. This suggests the potential application of TRIM23 for therapeutic and diagnostic purposes.

Materials and Methods

Cell Culture, Transfection, and Luciferase Reporter Assays. Details of cell culture, transfection, and luciferase reporter assays can be found in *SI Materials and Methods.*

Antibodies and Reagents. Antibodies and reagents are described in *SI Materials and Methods.*

Western Blotting and Immunoprecipitation. Details of Western blotting and immunoprecipitation are provided in *SI Materials and Methods.*

Knockdown. Knockdown details are given in *SI Materials and Methods.*

Microarray. Microarray details can be found in *SI Materials and Methods.*

Visual Analysis of Interaction. Details of visual analysis of interaction and bifluorescent complementation (Bifc) can be found in *SI Materials and Methods.*

ELISA. Culture medium from WT and TRAF6$^{-/-}$ MEFs were collected for the analysis of IFN-β production using mouse-specific ELISA kits (PBL Biomedical Laboratories).

cDNA Construction Details of cDNA construction can be found in *SI Materials and Methods.*

In Vitro Ubiquitination Assay. Assays details have been described previously (17). K27-only ubiquitin recombinant protein was purchased from Boston Biochem.

Assay of IRF3 Dimerization Details regarding assay of IRF3 dimerization are provided in *SI Materials and Methods.*

$TCID_{50}$ Assay. Approximate viral titers were calculated by 50% Tissue Culture Infectious Dose ($TCID_{50}$) assay. Further details can be found in *SI Materials and Methods.*

Statistical Methods. Statistical significance was determined by Student's *t* test.

ACKNOWLEDGMENTS. We thank Dr. Tak W. Mak (Ontario Cancer Institute, University Health Network) for the NEMO$^{-/-}$ and TRAF6$^{-/-}$ MEF cells; Dr. S. Akira (Osaka University, Osaka, Japan) for the TBK1$^{-/-}$IKKi$^{-/-}$ MEF cells; and Dr. Ritsuko Shiina, Dr. Hiromi Yabe, and Dr. Takayuki Hishiki (Chiba Institute of Technology, Chiba, Japan) for technical assistance. We are grateful to Dr. Takeshi Yoshida (Laboratory of Viral Pathogenesis, Kyoto University, Kyoto, Japan) for Bifc analysis. We thank Drs. Koichi Ikuta, Akira Shimizu, Manabu Sugai, Hiroshi Kadotani, and Fumihiko Matsuda (Graduate School of Medicine, Kyoto University) for providing an environment for experiments. This work was supported by grants-in-aid for Scientific Research on Priority Areas "Integrative Research Toward the Conquest of Cancer" from the Ministry of Education, Culture, Sports, Science and Technology of Japan. K-i.A. is a research fellow of the Japan Society for the Promotion of Science.

1. Akira S, Uematsu S, Takeuchi O (2006) Pathogen recognition and innate immunity. *Cell* 124:783–801.
2. Honda K, Takaoka A, Taniguchi T (2006) Type I interferon [corrected] gene induction by the interferon regulatory factor family of transcription factors. *Immunity* 25:349–360.
3. Kawai T, Akira S (2006) Innate immune recognition of viral infection. *Nat Immunol* 7: 131–137.
4. Stetson DB, Medzhitov R (2006) Type I interferons in host defense. *Immunity* 25:373–381.
5. Meylan E, Tschopp J, Karin M (2006) Intracellular pattern recognition receptors in the host response. *Nature* 442:39–44.
6. Yoneyama M, et al. (2004) The RNA helicase RIG-I has an essential function in double-stranded RNA-induced innate antiviral responses. *Nat Immunol* 5:730–737.
7. Meylan E, Tschopp J (2006) Toll-like receptors and RNA helicases: Two parallel ways to trigger antiviral responses. *Mol Cell* 22:561–569.
8. Kato H, et al. (2006) Differential roles of MDA5 and RIG-I helicases in the recognition of RNA viruses. *Nature* 441:101–105.
9. Kawai T, et al. (2005) IPS-1, an adaptor triggering RIG-I- and Mda5-mediated type I interferon induction. *Nat Immunol* 6:981–988.
10. Seth RB, Sun L, Ea CK, Chen ZJ (2005) Identification and characterization of MAVS, a mitochondrial antiviral signaling protein that activates NF-kappaB and IRF 3. *Cell* 122:669–682.
11. Meylan E, et al. (2005) Cardif is an adaptor protein in the RIG-I antiviral pathway and is targeted by hepatitis C virus. *Nature* 437:1167–1172.
12. Xu LG, et al. (2005) VISA is an adapter protein required for virus-triggered IFN-beta signaling. *Mol Cell* 19:727–740.
13. Saha SK, et al. (2006) Regulation of antiviral responses by a direct and specific interaction between TRAF3 and Cardif. *EMBO J* 25:3257–3263.
14. Kayagaki N, et al. (2007) DUBA: A deubiquitinase that regulates type I interferon production. *Science* 318:1628–1632.
15. Zhao T, et al. (2007) The NEMO adaptor bridges the nuclear factor-kappaB and interferon regulatory factor signaling pathways. *Nat Immunol* 8:592–600.
16. Gack MU, et al. (2007) TRIM25 RING-finger E3 ubiquitin ligase is essential for RIG-I-mediated antiviral activity. *Nature* 446:916–920.
17. Arimoto K, et al. (2007) Negative regulation of the RIG-I signaling by the ubiquitin ligase RNF125. *Proc Natl Acad Sci USA* 104:7500–7505.
18. Oshiumi H, Matsumoto M, Hatakeyama S, Seya T (2009) Riplet/RNF135, a RING finger protein, ubiquitinates RIG-I to promote interferon-β induction during the early phase of viral infection. *J Biol Chem* 284:807–817.
19. Chuang TH, Ulevitch RJ (2004) Triad3A, an E3 ubiquitin-protein ligase regulating Toll-like receptors. *Nat Immunol* 5:495–502.
20. Tanaka T, Grusby MJ, Kaisho T (2007) PDLIM2-mediated termination of transcription factor NF-kappaB activation by intranuclear sequestration and degradation of the p65 subunit. *Nat Immunol* 8:584–591.
21. Lin R, et al. (2006) Negative regulation of the retinoic acid-inducible gene I-induced antiviral state by the ubiquitin-editing protein A20. *J Biol Chem* 281:2095–2103.
22. Vichi A, Payne DM, Pacheco-Rodriguez G, Moss J, Vaughan M (2005) E3 ubiquitin ligase activity of the trifunctional ARD1 (ADP-ribosylation factor domain protein 1). *Proc Natl Acad Sci USA* 102:1945–1950.
23. Zhao H, et al. (2005) A novel E3 ubiquitin ligase TRAC-1 positively regulates T cell activation. *J Immunol* 174:5288–5297.
24. Gohda J, Matsumura T, Inoue J (2004) Cutting edge: TNFR-associated factor (TRAF) 6 is essential for MyD88-dependent pathway but not toll/IL-1 receptor domain-containing adaptor-inducing IFN-β (TRIF)-dependent pathway in TLR signaling. *J Immunol* 173:2913–2917.
25. Häcker H, et al. (2006) Specificity in Toll-like receptor signalling through distinct effector functions of TRAF3 and TRAF6. *Nature* 439:204–207.
26. Oganesyan G, et al. (2006) Critical role of TRAF3 in the Toll-like receptor-dependent and -independent antiviral response. *Nature* 439:208–211.
27. Nyman TA, Matikainen S, Sareneva T, Julkunen I, Kalkkinen N (2000) Proteome analysis reveals ubiquitin-conjugating enzymes to be a new family of interferon-alpha-regulated genes. *Eur J Biochem* 267:4011–4019.
28. Ye Y, Rape M (2009) Building ubiquitin chains: E2 enzymes at work. *Nat Rev Mol Cell Biol* 10:755–764.
29. Hochstrasser M (2006) Lingering mysteries of ubiquitin-chain assembly. *Cell* 124:27–34.
30. Koegl M, et al. (1999) A novel ubiquitination factor, E4, is involved in multiubiquitin chain assembly. *Cell* 96:635–644.
31. Zeng W, Xu M, Liu S, Sun L, Chen ZJ (2009) Key role of Ubc5 and lysine-63 polyubiquitination in viral activation of IRF3. *Mol Cell* 36:315–325.
32. Chen F, Bhatia D, Chang Q, Castranova V (2006) Finding NEMO by K63-linked polyubiquitin chain. *Cell Death Differ* 13:1835–1838.
33. Abbott DW, et al. (2007) Coordinated regulation of Toll-like receptor and NOD2 signaling by K63-linked polyubiquitin chains. *Mol Cell Biol* 27:6012–6025.
34. Ni CY, et al. (2008) Cutting edge: K63-linked polyubiquitination of NEMO modulates TLR signaling and inflammation in vivo. *J Immunol* 180:7107–7111.
35. Wu CJ, Conze DB, Li T, Srinivasula SM, Ashwell JD (2006) Sensing of Lys 63-linked polyubiquitination by NEMO is a key event in NF-kappaB activation [corrected]. *Nat Cell Biol* 8:398–406.
36. Tokunaga F, et al. (2009) Involvement of linear polyubiquitylation of NEMO in NF-kappaB activation. *Nat Cell Biol* 11:123–132.
37. Ashida H, et al. (2010) A bacterial E3 ubiquitin ligase IpaH9.8 targets NEMO/IKKgamma to dampen the host NF-kappaB-mediated inflammatory response. *Nat Cell Biol* 12:66–73, 1–9.

Pathology International

Pathology International 2010; **60**: 351–357 doi:10.1111/j.1440-1827.2010.02526.x

Original Article

Deregulation of miR-92a expression is implicated in hepatocellular carcinoma development

Masatoshi Shigoka,[1] Akihiko Tsuchida,[1] Takaaki Matsudo,[1] Yuichi Nagakawa,[1] Hitoshi Saito,[1] Yoshiaki Suzuki,[1] Tatsuya Aoki,[1] Yoshiki Murakami,[2] Hidenori Toyoda,[3] Takashi Kumada,[3] Ralf Bartenschlager,[4] Nobuyuki Kato,[5] Masanori Ikeda,[5] Tomoki Takashina,[6] Masami Tanaka,[6] Rieko Suzuki,[6] Kosuke Oikawa,[7] Masakatsu Takanashi[6] and Masahiko Kuroda[6]

[1]Third Department of Surgery and [6]Department of Molecular Pathology, Tokyo Medical University, Tokyo, Japan, [2]Center for Genomic Medicine, Kyoto University, Kyoto, Japan, [3]Department of Gastroenterology, Ogaki Municipal Hospital, Ogaki, Japan, [4]Department of Infectious Diseases, Molecular Virology, University of Heidelbergand, Heidelberg, Germany, [5]Department of Tumor Virology, Okayama University Graduate School of Medicine, Okayama, Japan, and [7]First Department of Pathology, Wakayama Medical University, Wakayama, Japan

MicroRNAs (miRNAs) belong to a class of the endogenously expressed non-coding small RNAs which primarily function as gene regulators. Growing evidence suggests that miRNAs have a significant role in tumor development and may constitute robust biomarkers for cancer diagnosis and prognosis. The *miR-17-92* cluster especially is markedly overexpressed in several cancers, and is associated with the cancer development and progression. In this study, we have demonstrated that miR-92a is highly expressed in hepatocellular carcinoma (HCC). In addition, the proliferation of HCC-derived cell lines was enhanced by miR-92a and inhibited by the anti-miR-92a antagomir. On the other hand, we have found that the relative amount of miR-92a in the plasmas from HCC patients is decreased compared with that from the healthy donors. Interestingly, the amount of miR-92a was elevated after surgical treatment. Thus, although the physiological significance of the decrease of miR-92a in plasma is still unknown, deregulation of miR-92 expression in cells and plasma should be implicated in the development of HCC.

Key words: hepatocellular carcinoma, microRNA, miR-638, miR-92a, plasma

Correspondence: Masahiko Kuroda, MD, PhD, Department of Molecular Pathology, Tokyo Medical University, 6-1-1 Shinjuku, Shinjuku-ku, Tokyo 160-8402, Japan. Email: kuroda@tokyo-med.ac.jp

Received 8 November 2009. Accepted for publication 23 December 2009.

MicroRNAs (miRNAs) are small endogenous non-coding RNAs that regulate gene expression and have a critical role in many biological and pathological processes.[1] Recent studies have shown that deregulation of miRNA expression contributes to the multistep processes of carcinogenesis, and have shown promise as tissue-based markers for cancer classification and prognostication.[2,3] However, biological roles of only a small fraction of known miRNAs have been elucidated to date.

The miR-17-92 cluster at 13q31.3 is consists of six miRNAs: miR-17, miR-18a, miR-19a, miR-20a, miR-19b-1 and miR-92a-1, and plays an important role for development of lung cancer,[4] B-cell lymphomas,[5] chronic myeloid leukemia,[6] medulloblastomas,[7] colon cancer[8] and hepatocellular carcinoma (HCC).[9] In addition, mice deficient in the miR-17-92 cluster died shortly after birth with lung hypoplasia, and B-cell development was impaired in the mice.[10] It has been reported, however, that miR-92a increases cell proliferation by negative regulation of an isoform of the cell-cycle regulator p63.[11] Furthermore, miR-92a regulates angiogenesis.[12] Thus, it is clear that the miR-92a has some oncogenic characteristics. However, the specific biological role of miR-92a in the processes of human cancer development has remained unclear.

Here, we have revealed that miR-92a is implicated in human HCC development. Furthermore, we have demonstrated that miR-92a in human blood has the potential to be a noninvasive molecular marker for diagnosis of human HCC.

MATERIALS AND METHODS

In situ hybridaization of miR-92a

Locked nucleic acid (LNA)-modified probes for miR-92a and negative control (miRCURY-LNA detection probe, Exiqon, Vedbaek, Denmark) were used. The probe sequences were as follows; *miR-92a*, 5′-ACAGGCCGGGACAAGTGCAATA-3′; and a scrambled oligonucleotides used for negative control, 5′-GTGTAACACGTCTATACGCCCA-3′. *In situ* hybridization was performed using the RiboMap *in situ* hybridization kit (Ventana Medical Systems, Tucson, AZ, USA) on the Ventana Discovery automated *in situ* hybridization instrument (Ventana Medical Systems). The *in situ* hybridization steps were performed as previously described.[13] Staining was evaluated by two investigators and graded as follows: negative (–), no or occasional (<5%) staining of tumor cells; positive (+), mild to strong (>5%) staining of tumor cells. Paraffin–embedded tissue samples of hepatocellular carcinoma (HCC) and adjacent non-tumorous liver cirrhosis (LC) were obtained from HCC patients at Ogaki Municipal Hospital (Ogaki, Japan). Details of the clinical data are provided in Table 1.

Plasma collection, RNA isolation and quantitative RT-PCR

Whole blood samples were collected from healthy donors and the patients with HCC at Ogaki Municipal Hospital. This study was approved by the institutional review board (IRB) of Tokyo Medical University, and all subjects provided written informed consent under the institutional review board. Details of clinical data are provided in Table 1. Diagnoses were confirmed using the post-operated tissues. Blood samples of the patients (Cases 1–10) were collected one day before the operation and then properly stored. One week after operation, blood samples of the patients were collected again. Whole blood was separated into plasma and cellular fractions by centrifugation at 1600 *g* for 15 min. Total RNA in the

Table 1 Summary of clinical details of hepatocellular carcinoma (HCC)used for in situ hybridaization and serum analysis

	Year	Sex	Virus type	Histologic type	Stage	Child-Pugh	miR-92a
Case 1	53	Male	HBV	Poorly	I	A	+
Case 2	59	Male	HBV	Moderate	II	A	+
Case 3	79	Male	NBNC	Moderate	III	A	+
Case 4	73	Male	HCV	Well	I	A	+
Case 5	76	Female	HCV	Moderate	IV-A	A	+
Case 6	59	Male	HCV	Moderate	II	A	+
Case 7	69	Female	HCV	Moderate	I	A	+
Case 8	71	Male	HCV	Moderate	I	A	+
Case 9	59	Female	HBV	Well	I	A	–
Case 10	69	Male	NBNC	Moderate	IV-A	A	–
Case 11	61	Female	HBV	Poorly	IV-A	B	+
Case 12	73	Male	NBNC	Moderate	II	A	+
Case 13	67	Male	NBNC	Moderate	IV-A	A	+
Case 14	61	Male	NBNC	Moderate	III	A	+
Case 15	45	Male	HBV	Moderate	I	A	+
Case 16	68	Female	HCV	Moderate	III	A	+
Case 17	70	Male	NBNC	Poorly	II	A	+
Case 18	59	Male	HCV	Moderate	III	A	+
Case 19	43	Male	HBV	Moderate	II	A	+
Case 20	69	Male	HCV	Moderate	II	A	–
Case 21	76	Male	HCV	Moderate	III	A	–
Case 22	53	Male	HCV	Moderate	II	A	–

HCV, hepatitis C virus; HBV, hepatitis B virus; NBNC, non-B non-C virus.

Table 2 Summary of clinical details of hepatocellular carcinoma (HCC) used for qPCR analysis

Code no.	Year	Sex	Virus type	Histologic type	Non-tumorous tissue	AFP	PIVKA-II
91	53	Male	HCV	Moderate	LC	5	0.06
160	59	Male	HCV	Moderate	LC	NI	NI
O89	68	Male	HCV	Moderate	LC	8	25
O90	70	Male	HCV	Moderate	LC	686	962
K89	51	Male	HCV	Moderate	LC	NI	NI

LC, liver cirrhosis; HCV, hepatitis C virus; NI, no information.

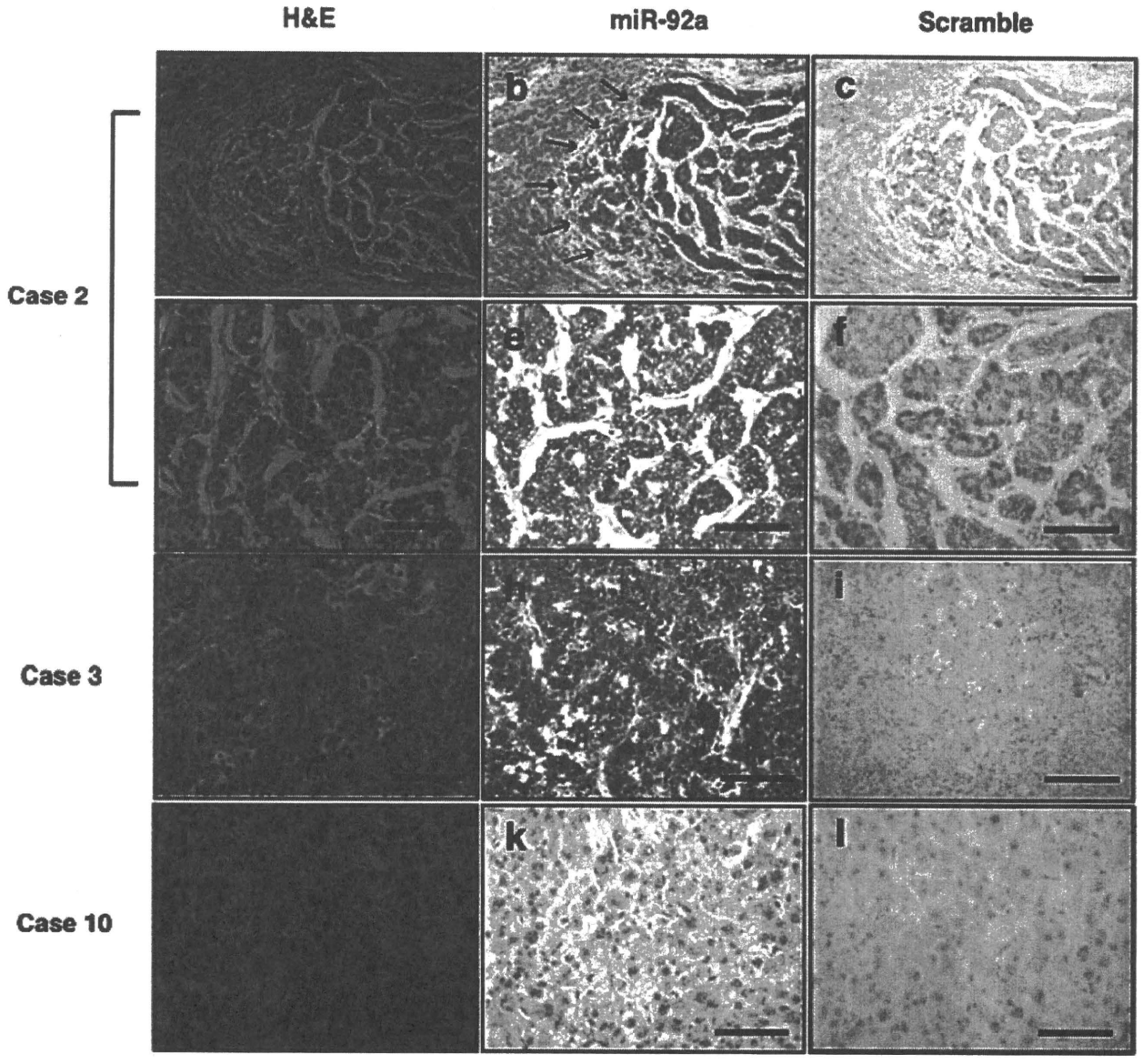

Figure 1 MiRNA expression in hepatocellular carcinoma (HCC). *In situ* hybridization was performed using Locked nucleic acid (LNA)-modified probes for miR-92a and negative control. Case 2 and Case 3 were positive cases for miR-92a. Case 10 was a negative case for miR-92a. (**a–c**) Low power field of boundary of HCC and non-tumor lesion. Arrowheads indicated a border. Only HCC regions were positive for miR-92a. (**d–l**) High power field of HCC. Blue signals represent positive for miR-92a. Bars indicate 100 μm.

plasma was isolated using Isogen-LS (NIPPON GENE, Tokyo, Japan) according to the manufacturer's instructions. The RNA sample was suspended in 20 μL of nuclease free water. In general, we obtained 400 ng of RNA from 1 mL of plasma. MiRNAs were quantified using TaqMan MiRNA Assays (Applied Biosystems, Life Technologies Corporation, Carlsbad, CA, USA) as previously described.[13]

For miR-92a quantification in tissue samples, five pairs of fresh HCC and non-tumorous LC samples were surgically resected from HCC patients (Table 2). All the patients or their guardians provided written informed consent, and the Ethics Committee of the Kyoto University Graduate School and Faculty of Medicine approved all aspects of this study. The amounts of miR-92a were normalized to RNU48 that is one of rRNAs (Applied Biosystems).

Cell culture and transfection

Hepatocellular carcinoma (HCC) cell lines HepG2, OR6 and SN1a were cultured in Dulbecco's modified Eagle's medium

(DMEM) (Sigma, St. Louis, MO, USA) supplemented with 10% fetal bovine serum (FBS). OR6 and SN1a are derived from the Huh7 HCC cell line and maintain hepatitis C virus (HCV) replicon.[14–16] The miR-92a oligonucleotide used in the transfection experiments is a synthetic double-strand 19 nucleotide RNA oligonucleotide (5′-UUGCACUUGUCCC GGCCUG-3′) purchased from B-Bridge International (Tokyo, Japan). The scrambled oligonucleotide represents a mix of two different frames of the miR-92 sequence (5′-UAUUGC ACUUGUCCCGGCCUGUCCCGGCC-3′ and 5′-AUUGCAC UUGUCCCGGCCUTT-3′). Locked nucleic acid (LNA) oligonucleotide miR-92 knockdown (antagomir) was obtained from Exiqon (Vedbaek, Denmark, http://www.exiqon.com). The oligonucleotides were individually transfected by Hiper-Fect (QIAGEN K. K., Tokyo, Japan) into the cells at a final concentration of 100 nM.

In vitro proliferation assays

The effects of miR-92a and the anti-miR-92a antagomir on the growth of HepG2, OR6 and SN1a were evaluated using the MTT cell growth assay kit (Cell Count Reagent SF, Nacalai tesque, Kyoto, Japan). The cells were transfected with miR-92a or the antagomir. The cell numbers were then assessed with MTT assay at 48 or 72 h after the transfection. The MTT assay was performed according to the manufacturer's recommendation. The reagents were added to each well and incubated at 37°C for 4 h. The MTT reduced by living cells into a formazan product was assayed with a multiwell scanning spectrophotometer at 450 nm.

RESULTS

Highly expression of miR-92a in HCC cells

We first examined whether or not miR-92a is expressed in hepatocellular carcinoma (HCC). We performed *in situ* hybridization using locked nucleic acid (LNA)-modified probes digoxigenin (DIG) labelled. We found that miR-92a was strongly expressed in cancer cells of 17 out of 22 HCC cases (Table 1 and Fig. 1). No significant differences were observed in age, sex, virus type, clinical stage and tumor differentiation of the clinical samples. In contrast, we did not detect miR-92a expression in non-cancerous hepatocytes around the HCCs.

Furthermore, we quantified miR-92a levels in HCC sections ($n = 5$) and their adjacent non-tumorous liver cirrhosis (LC) sections ($n = 5$) by *Taq*Man qRT-PCR (Table 2 and Fig. 2). The levels of miR-92a expression in HCC sections were higher than that in adjacent LC sections (Fig. 2).

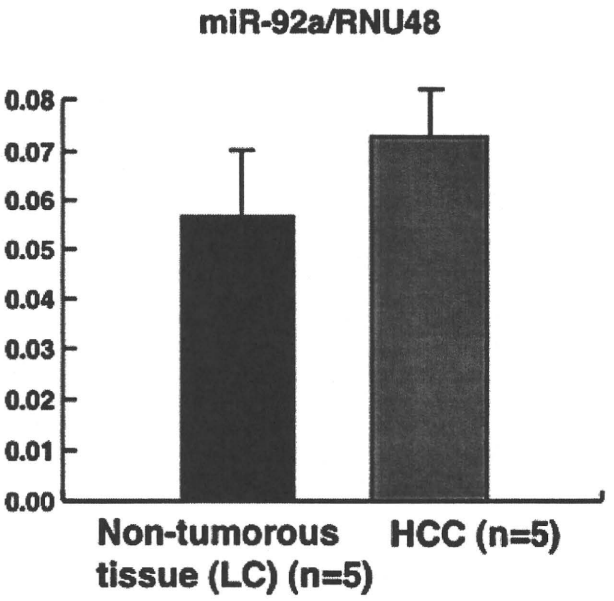

Figure 2 Quantification of miR-92a expression in hepatocellular carcinoma (HCC) tissue samples. The ratios of miR-92a to RNU48 in HCC tissues and their adjacent non-tumorous liver cirrhosis (LC) tissues were analyzed by *Taq*Man qRT-PCR. *Bars*, s.d.

Effects of miR-92a on a Hepatoma cell lines HepG2, OR6 and SN1a

Next, we investigated whether miR-92a affects cell proliferation of human HCC cell lines, HepG2, OR6 and SN1a. We transiently transfected either miR-92a or the anti-miR-92a antagomir into the cells. Antagomirs are single-stranded RNAs that are complementary to a specific miRNA and cause the depletion of the miRNA.[17] After the transfection, we found that all of the cells transfected with the anti-miR-92a antagomir showed lower proliferation rate than the cells transfected with a control RNA oligonucleotide (Fig. 3a). In contrast, the cells except for HepG2 showed increased proliferation rate when miR-92a was transfected (Fig. 3a). We also confirmed the amounts of miR-92a in the cells by quantitative real time PCR (Fig. 3b).

The ratio of miR-92a to miR-638 serves as a biomarker for HCC

Finally, we sought to determine whether the expression level of miR-92a in blood sera could discriminate HCC patients from healthy individuals. Previously, we have revealed that miR-92a is dramatically reduced in the plasmas of acute leukemia patients although in leukemic cells it is strongly expressed.[13] We analyzed the miR-92a levels in the plasma samples from normal individuals ($n = 10$) and HCC patients

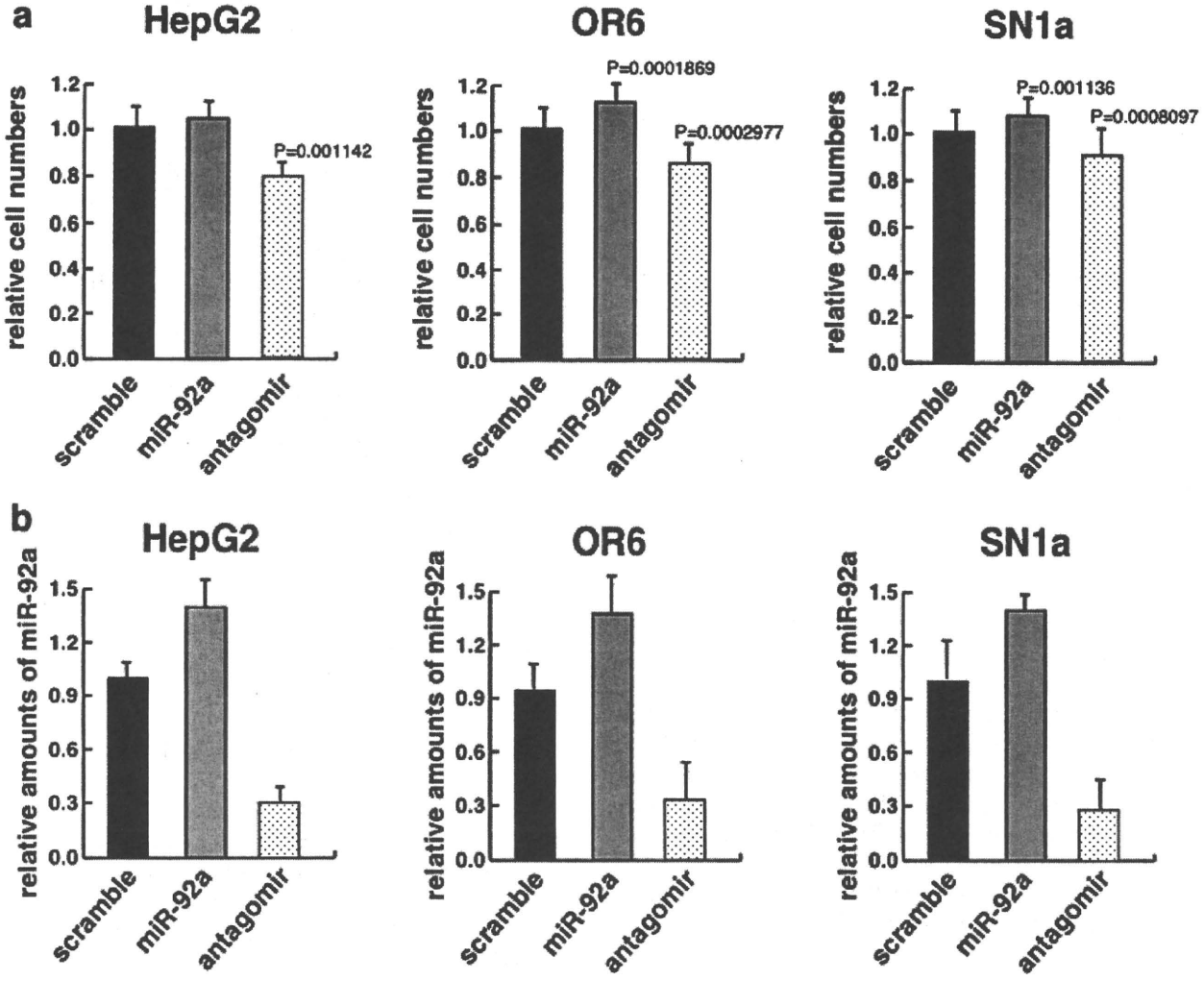

Figure 3 miR-92a modulates proliferation of HepG2, OR6 and SN1a cells. (**a**) Cell numbers of the HepG2, OR6 and SN1a cells transfected with synthetic miR-92a, anti-miR-92a antagomir, or scrambled control oligonucleotide were analyzed by MTT assays at 48 h for OR6 and SN1a and 72 h for HepG2 after transfection. *Bars*, s.d. (**b**) qRT-PCR analysis of miR-92a amounts in the cells transfected with miR-92a, anti-miR-92a antagomir or scrambled control at 48 h for OR6 and SN1a and 72 h for HepG2 after the transfection.

(n = 10) by *Taq*Man qRT-PCR. Because miR-638 is stably present in human plasmas,[13] we used miR-638 as the standard to improve the precision of the data. The ratio of miR-92a to miR-638 in the plasma samples from the HCC patients were decreased compared with that from the normal donors (Fig. 4a). Then, we further examined the ratio from the patients after surgical resection. Interestingly, the miR-92a/miR-638 levels were significantly higher than that in the plasmas from the patients before surgical resection (Fig. 4b).

DISCUSSION

In this study, we found that miR-92a was highly expressed in HCC (Figs 1,2). In addition, we demonstrated that the expression level of miR-92a affects the proliferation of hepatoma cell lines, HepG2, OR6 and SN1a (Fig. 3). These results suggest that miR-92a may play an important role in tumor progression of hepatocyte. We do not know why, but addition of miR-92a did not significantly increase the proliferation of HepG2 cells. It may be possible that HepG2 cells themselves already contain enough miR-92a to promote cancer cell proliferation. In addition, miR-92a is a part of the miR-17-92 cluster, which is actively involved in the development and progression of various cancers.[4–10] However, the molecular function of miR-92a is still unknown, and its mRNA targets have not been identified. Recently, it has been shown that one of the molecular mechanisms through which miR-92a increases cell proliferation is by negative regulation of an isoform of the cell-cycle regulator p63.[11] Thus, we examined

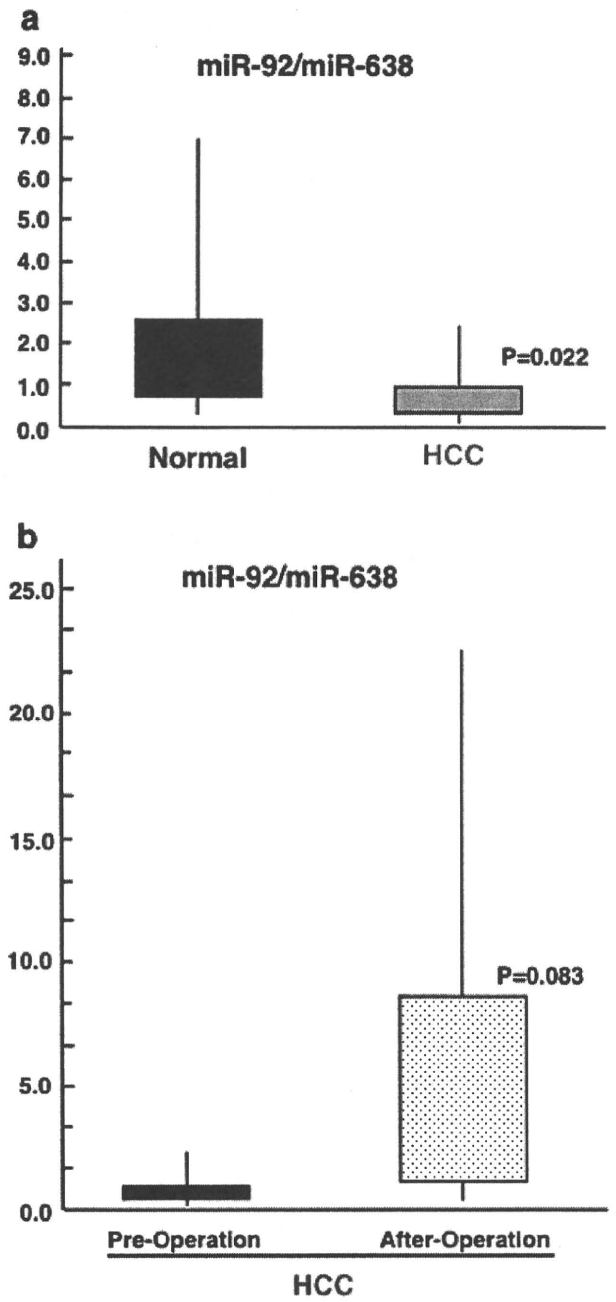

Figure 4 Comparison of miR-92a levels in the plasmas from normal individuals and hepatocellular carcinoma (HCC) patients. (**a**) The ratios of miR-92a to miR-638 in the plasmas from normal donors and HCC patients were analyzed by *Taq*Man qRT-PCR. Student's *t*-test was used to determine statistical significance. (**b**) The ratios of miR-92a to miR-638 in the plasmas from HCC patients before and after tumor resection were analyzed by *Taq*Man qRT-PCR.

the expression of p63 in HCC by immunohistochemistry. However, we could not find the positive nuclear staining both in HCC and normal hepatocyte (data not shown). On the other hand, the miRanda software found 300 different genes that have putative miR-92a binding sites conserved among *Homo sapiens*, *Mus musculus*, and *Rattus norvegicus* at the 3′-UTR regions of their transcripts. Therefore, at least in HCC, there may be novel miR-92a targets that are involved in cancer cell proliferation.

In this report, we have revealed that the value of miR-92a/miR-638 in plasma has potential as a very sensitive marker for HCC. We found that the ratio of miR-92a to miR-638 in the plasma samples from the HCC patients were decreased compared with that from the normal donors (Fig. 4a). We did not find any differences in the values of the ratios between hepatitis B virus (HBV) infection and hepatitis C virus (HCV) infection (data not shown). On the other hand, we recently observed decrease of miR-92a in plasma samples of acute leukemia.[13] These results suggest that the decrease of the miR-92a/miR-638 level in human plasma may serve as a valuable diagnostic marker for not only acute leukemia but also solid tumors such as HCC. Moreover, we observed increase of miR-92a/miR-638 levels in the plasmas from the HCC patients after tumor resection (Fig. 4b). Thus, the miR-92a/miR-638 levels in human plasmas may also be a potential noninvasive follow up marker of HCC. To confirm this notion, a large number of plasma samples should be examined. Nevertheless, the levels of miR-92a/miR-638 promise to be an effective biomarker for malignant tumors. The physiological significance of the decrease of miR-92a in plasma is still unknown.

In summary, we have shown that miR-92a may be involved in HCC development. In addition, we have demonstrated that the ratio of miR-92a/miR-638 in blood is expected to be useful for diagnosis of HCC patients. This study may also provide useful information for further investigations of functional association between miRNAs and HCC.

ACKNOWLEDGMENTS

This work was supported by Grants-in-Aids from the Ministry of Education, Culture, Sports, Science and Technology of Japan, the Ministry of Health, Labour and Welfare of Japan, Japan Health Sciences Foundation and a grant of Yamaguchi Endocrine Research Association and the grant of 'University-Industry Joint Research Project' for private universities as well as a matching fund subsidy from the MEXT (Ministry of Education, Culture, Sports, Science and Technology, 2007–2009). We thank Koji Fujita for his technical assistance and Satoko Aochi for her outstanding editorial assistance.

REFERENCES

1 Mattick JS, Makunin IV. Non-coding RNA. *Hum Mol Genet* 2006; **15** (Spec No. 1): R17–29.